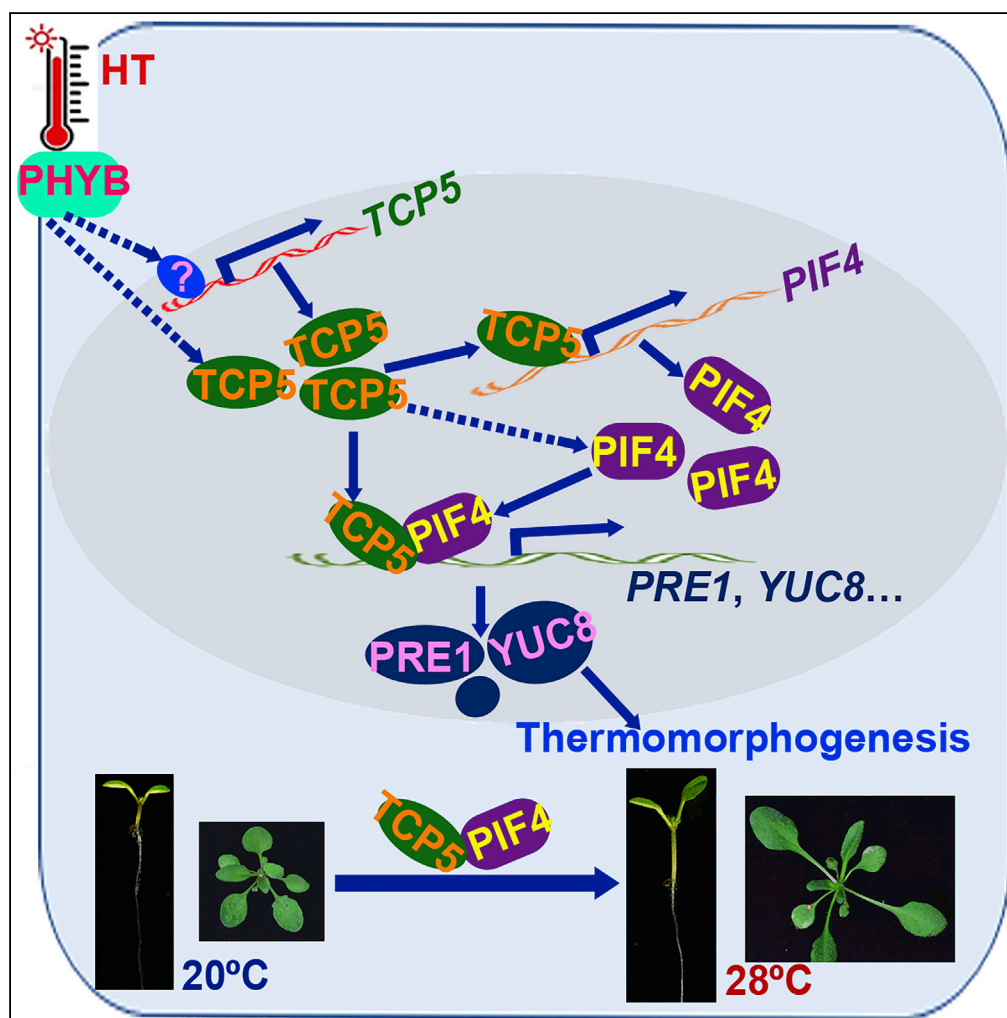


## Article

# *Arabidopsis* Transcription Factor TCP5 Controls Plant Thermomorphogenesis by Positively Regulating PIF4 Activity



Xiang Han, Hao Yu, Rongrong Yuan, Yan Yang, Fengying An, Genji Qin

qingenji@pku.edu.cn

#### HIGHLIGHTS

TCP5, TCP13, and TCP17 positively regulate plant thermomorphogenesis

TCP5 directly interacts with PIF4 transcription factor

TCPs and PIF4 share common downstream target genes

TCP5 promotes PIF4 activity at both transcriptional and protein levels

Han et al., iScience 15, 611–622  
 May 31, 2019 © 2019 The Author(s).  
<https://doi.org/10.1016/j.isci.2019.04.005>

## Article

# *Arabidopsis* Transcription Factor TCP5 Controls Plant Thermomorphogenesis by Positively Regulating PIF4 Activity

Xiang Han,<sup>1,3,4</sup> Hao Yu,<sup>1</sup> Rongrong Yuan,<sup>1,3,4</sup> Yan Yang,<sup>1,5</sup> Fengying An,<sup>1</sup> and Genji Qin<sup>1,2,6,\*</sup>

## SUMMARY

Plants display thermomorphogenesis in response to high temperature (HT). PHYTOCHROME INTERACTING FACTOR 4 (PIF4) is a central integrator regulated by numerous negative regulators. However, the mechanisms underpinning PIF4 positive regulation are largely unknown. Here, we find that TEOSINTE BRANCHED 1/CYCLOIDEA/PCF 5 (TCP5), TCP13, and TCP17 transcription factors promote the activity of PIF4 at transcriptional and post-transcriptional levels. TCP5 is rapidly induced by HT treatment, and TCP5 protein stability increases under HT. The overexpression of TCP5 causes constitutive thermomorphogenic phenotypes, whereas the *tcp5 tcp13 tcp17* triple mutant exhibits aberrant thermomorphogenesis. We demonstrate that TCP5 not only physically interacts with PIF4 to enhance its activity but also directly binds to the promoter of PIF4 to increase its transcript. TCP5 and PIF4 share common downstream targets. The *tcp5 tcp13 tcp17* mutant partially restores the long hypocotyls caused by PIF4 overexpression. Our findings provide a layer of understanding about the fine-scale regulation of PIF4 and plant thermomorphogenesis.

## INTRODUCTION

The strong 2018 summer heat waves across the Northern Hemisphere caused a high temperature (HT) of up to 30°C in some areas of the Arctic Circle and also severe losses in crop production. There is an urgent need to elucidate the molecular mechanisms by which plants adapt to HT. Plant thermomorphogenesis refers to changes in plant growth, development, and morphology under HT (Stavang et al., 2009). These changes, including hypocotyl elongation, petiole elongation, and hyponastic growth, are important for plant survival under HT (Quint et al., 2016; Wigge, 2013). The basic-helix-loop-helix (bHLH) transcription factor PHYTOCHROME INTERACTING FACTOR 4 (PIF4) integrates HT and other environmental cues with hormonal signals and acts as a central hub in the control of thermomorphogenesis (Franklin et al., 2011; Koini et al., 2009; Sun et al., 2012), and its activity is tightly regulated by numerous negative regulators (Bernardo-Garcia et al., 2014; Box et al., 2015; Delker et al., 2014; Foreman et al., 2011; Gangappa and Kumar, 2017; Jung et al., 2016; Legris et al., 2016; Ma et al., 2016; Nieto et al., 2015; Nusinow et al., 2011; Somers et al., 1991; Song et al., 2017; Tasset et al., 2018; Toledo-Ortiz et al., 2014; Zhang et al., 2017, 2018). At the transcriptional level, PIF4 transcripts are negatively regulated by the light-signaling component LONG HYPOCOTYL 5 (HY5) (Gangappa and Kumar, 2017; Toledo-Ortiz et al., 2014) and the evening complex component EARLY FLOWERING 3 (ELF3) (Nieto et al., 2015; Nusinow et al., 2011). At the protein level, the phosphorylation of PIF4, which is required for its degradation, is mediated by the BRASSINOSTEROID-INSENSITIVE 2 (BIN2) kinase in brassinosteroid (BR) signaling and by phytochrome B (phyB), which acts as both a photoreceptor and a thermosensor (Bernardo-Garcia et al., 2014; Jung et al., 2016; Legris et al., 2016; Song et al., 2017). Recently, BLADE-ON-PETIOLE (BOP) proteins, a component of CUL3<sup>BOP1/BOP2</sup> (CULLIN3A<sup>BOP1/BOP2</sup>) E3 ubiquitin ligase complex, have been reported to mediate PIF4 degradation (Zhang et al., 2017). Several proteins, such as CRYPTOCHROME 1 (CRY1) (Ma et al., 2016), LONG HYPOCOTYL IN FAR-RED 1 (HFR1) (Foreman et al., 2011), and ELF3 (Box et al., 2015), repress PIF4 transcriptional activity by directly interacting with PIF4. However, to date, apart from BRASSINAZOLE RESISTANT 1 (BZR1) (Ibanez et al., 2018; Oh et al., 2012, 2014), very few PIF4 positive regulators have been found. Our previous work has found that *Arabidopsis* transcriptional repressor SPOROXYTELESS/NOZZLE (SPL/NZZ) inhibits the activity of CININNATA (CIN)-like TCP family and that the overexpression of TCP5 leads to aborted ovules (Wei et al., 2015). TCP proteins are a conserved, plant-specific class of transcription factors (Martín-Trillo and Cubas, 2010). They are further grouped into Class I and Class II based on their conserved TCP domains, which are responsible for DNA binding or protein-protein interactions (Martín-Trillo and Cubas, 2010). TCPs play essential roles in the control of plant development (Aggarwal et al.,

<sup>1</sup>State Key Laboratory of Protein and Plant Gene Research, School of Life Sciences, Peking University, Beijing 100871, The People's Republic of China

<sup>2</sup>School of Advanced Agricultural Sciences, Peking University, Beijing 100871, People's Republic of China

<sup>3</sup>The Peking-Tsinghua Center for Life Sciences, Beijing 100871, The People's Republic of China

<sup>4</sup>Academy for Advanced Interdisciplinary Studies, Peking University, Beijing 100871, The People's Republic of China

<sup>5</sup>Academy for Advanced Interdisciplinary Studies, Southern University of Science and Technology (SUSTech), Shenzhen 518055, China

<sup>6</sup>Lead Contact

\*Correspondence:

qingenji@pku.edu.cn

<https://doi.org/10.1016/j.isci.2019.04.005>



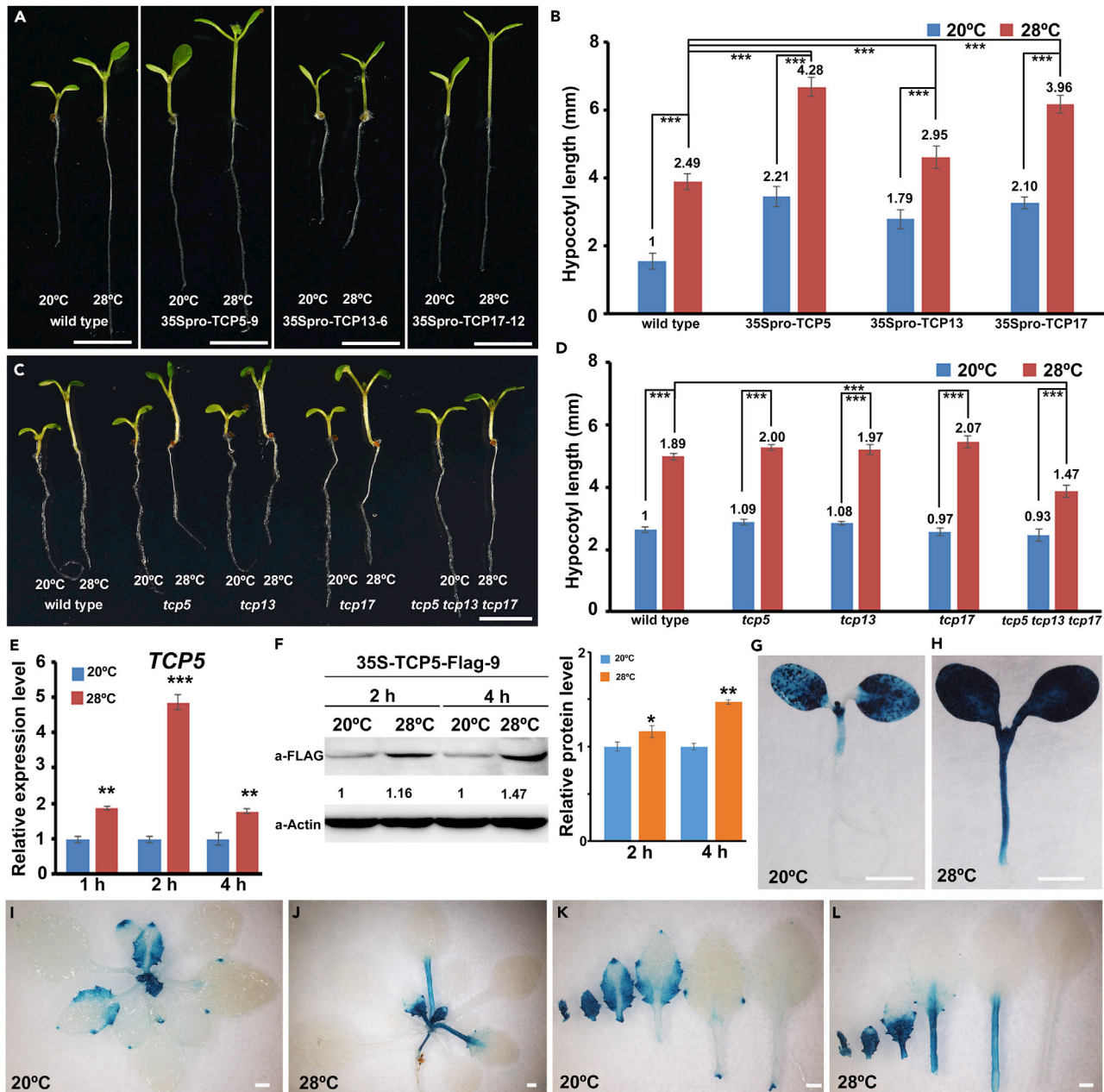


**Figure 1. TCP5 Regulates Plant Thermomorphogenesis**

(A) Phenotypes of 10-day-old wild-type, 35Spro-TCP5-9, 35Spro-TCP13-6, and 35Spro-TCP17-12 seedlings grown continuously at 20°C for 7 days before being transferred to 28°C for 3 days.

(B) Statistical analysis of the hypocotyl lengths of the plants in (A).

(C) Phenotypes of 10-day-old wild-type, *tcp5*, *tcp13*, *tcp17*, and *tcp5 tcp13 tcp17* triple mutant seedlings after HT treatment. (D) Statistical analysis of the hypocotyl lengths of the plants in (C).

(B and D) Data represent the mean  $\pm$  SD of three biological replicates. Significant differences are indicated with \* $p < 0.05$ ,  $n > 20$ , two-tailed Student's *t* test; \*\* $p < 0.01$ ; \*\*\* $p < 0.001$ . The number above each column indicates fold changes of hypocotyl length relative to wild-type control under 20°C.

(E) Relative expression levels of *TCP5* in wild-type after HT treatment for 1, 2, or 4 h. The expression levels of *TCP5* were normalized to that of *ACT8* and were relative to that in wild-type grown under normal temperatures. Data represent the mean  $\pm$  SD of three biological replicates.

(F) Stability of TCP5 protein under HT treatment. 35Spro-TCP5-FLAG plants were treated with HT for 2 and 4 h.

(G and H) GUS staining of 10-day-old TCP5pro-GUS transgenic seedlings after treatment. Seven-day-old TCP5pro-GUS seedlings grown under continuous 20°C before being transferred to 20°C (G) or 28°C (H) for 3 additional days of growth.

**Figure 1. Continued**

(I) GUS staining of 26-day-old TCP5pro-GUS plants grown under normal temperature.

(J) GUS staining of 26-day-old TCP5pro-GUS plants treated with HT for 5 days.

(K) Close-up view of dissected leaves from (I).

(L) Close-up view of dissected leaves from (J).

Scale bars, 5 mm in (A and C) and 1 mm in (G–L). See also Figure S1.

2010; Aguilar-Martinez et al., 2007; Efroni et al., 2008; Gonzalez-Grandio et al., 2013; Kieffer et al., 2011; Koyama et al., 2007, 2010; Nath et al., 2003; Palatnik et al., 2003; Yang et al., 2018), such as internode length (Kieffer et al., 2011), leaf shape (Efroni et al., 2008; Koyama et al., 2007, 2010), and axillary branching (Aguilar-Martinez et al., 2007; Gonzalez-Grandio et al., 2013). However, TCPs have not been found to be participating in the regulation of plant thermomorphogenesis yet. Here, we show that TCP5, TCP13, and TCP17 act as positive regulators in plant response to HT. Overexpression of *TCP5*, *TCP13*, or *TCP17* leads to constitutive thermomorphogenesis, whereas the triple mutant *tcp5tcp13tcp17* displays aberrant thermomorphogenesis. TCP5 is accumulated under HT and directly interacts with the central regulator PIF4. We finally demonstrate that TCP5 plays an essential role in plant thermomorphogenesis by promoting the activity of PIF4 at both transcriptional and post-transcriptional levels.

**RESULTS AND DISCUSSION****TCP5 Positively Regulates Plant Thermomorphogenesis**

We previously found that the overexpression of *TCP5* leads to aborted ovules (Wei et al., 2015). Surprisingly, we observed that most 35Spro-TCP5 overexpression lines (32/41) displayed constitutive thermomorphogenesis, including long hypocotyls, long petioles, and increased leaf hyponasty under normal temperatures (Figures 1A, 1B, and S1A–S1E), implying that TCP5 might play important roles in plant thermomorphogenesis. The protein alignments suggest that TCP5 is highly similar to TCP13 and TCP17, and that they form a small clade in the Class II TCP family (Figures S1F and S1G). To test whether TCP13 and TCP17 could be functionally redundant with TCP5, we overexpressed *TCP13* or *TCP17* using the Cauliflower Mosaic Virus (CaMV) 35S promoter and found that both 35Spro-TCP13 and 35Spro-TCP17 transgenic plants exhibited longer hypocotyls at 20°C and 28°C, resembling the constitutive thermomorphogenesis observed in 35Spro-TCP5 plants (Figures 1A and 1B). We then investigated the hypocotyl lengths of *tcp5*, *tcp13*, and *tcp17* single mutants and of a *tcp5tcp13tcp17* triple mutant under 28°C treatment for 3 days. The single mutants displayed no differences from the wild-type in hypocotyl length at 20°C or 28°C, whereas the triple mutant produced shorter hypocotyls than the wild-type under 28°C (Figures 1C and 1D). We further found that the petiole length of *tcp5 tcp13 tcp17* was shorter than that of the wild-type under 28°C (Figures S1H and S1I), indicating that *tcp5 tcp13 tcp17* mutants were insensitive to HT treatment. These results demonstrate that TCP5 has functional redundancy with TCP13 and TCP17 in the positive regulation of plant thermomorphogenesis.

**HT Regulates TCP5 at Transcriptional and Post-transcriptional Levels**

To test whether the expression level of *TCP5*, *TCP13*, and *TCP17* could be regulated by HT, we first treated wild-type *Arabidopsis* seedlings with HT in a time course (1, 2, or 4 h). Quantitative real-time PCR (qRT-PCR) assays showed that the transcripts of *TCP5*, *TCP13*, and *TCP17* were all rapidly induced by HT (Figures 1E, S1J, and S1K). PIF4 is a central regulator in plant response to HT (Franklin et al., 2011; Koini et al., 2009; Sun et al., 2012). We then tested the expression levels of *TCP5* in *pif4* mutant with or without HT treatment. The results showed that the induction of *TCP5* in HT was significantly reduced (Figure S1L). We further investigated TCP5 protein stability using 35Spro-TCP5-FLAG transgenic plants. The results indicated that TCP5 was more stable under HT than under normal conditions (Figure 1F). To investigate the expression pattern of *TCP5*, we generated a TCP5pro-GUS construct in which the *GUS* reporter gene was driven by the 2,400-bp *TCP5* promoter. Fifteen TCP5pro-GUS transgenic lines showed similar GUS staining patterns, and strong GUS activity was observed in the cotyledons, hypocotyls, young leaf blades, and petioles (Figures 1G, 1I, 1K, and S1M–S1O). As the leaves grew, GUS staining gradually faded from the petioles and from the middle region of the blades to the leaf margins, which were mainly restricted to the leaf margins or serrations (Figures 1I, 1K, S1N, and S1O). GUS staining was also observed in the petals, anthers, pistils, and siliques (Figures S1P and S1Q). In addition, we also detected GUS signals in ovule and pollen grains in TCP5pro-GUS transgenic plants (Figures S1R and S1S). Furthermore, 28°C HT treatment for 3 days strengthened the GUS activity in the hypocotyls and cotyledons of TCP5pro-GUS-4 plants (Figures 1G and 1H). Interestingly, HT treatment for 3 days led to strong GUS activity shifting from the leaf blades to

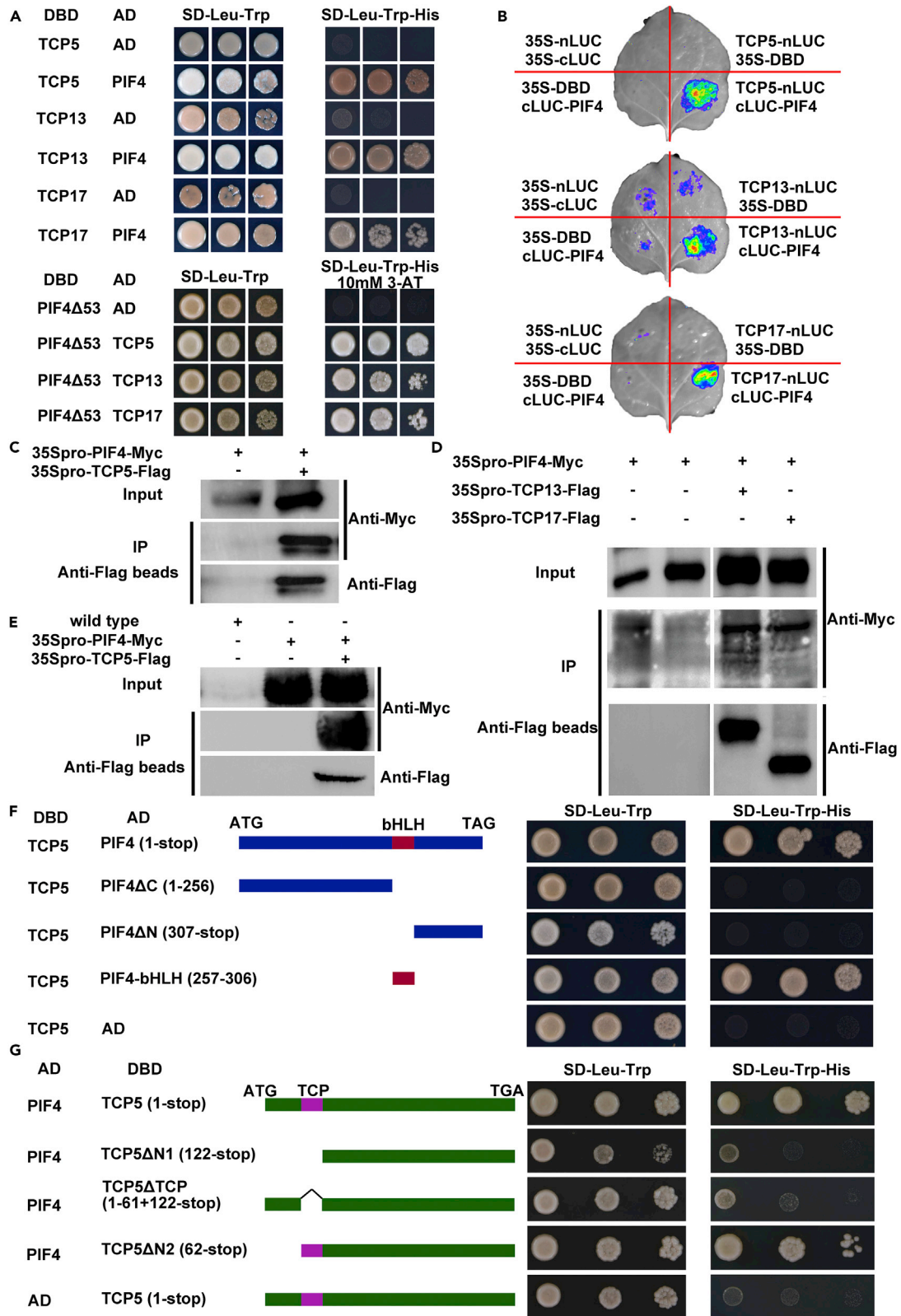


### Figure 2. TCP5 Interacts with PIF4

(A) Yeast two-hybrid assays showing that TCP5, TCP13, and TCP17 interact with PIF4. The DNA-binding domain (DBD) was fused to TCPs or truncated PIF4 $\Delta$ 53, in which 53 amino acids at the N-terminal end were deleted. The activation domain (AD) was fused to PIF4 or TCPs. Co-transformed yeast cells were grown on medium lacking Leu and Trp (SD-Leu-Trp) and selected on medium lacking Leu, Trp, and His (SD-Leu-Trp-His) with or without 10 mM 3-amino-1,2,4 triazole (3-AT) at dilutions of 10- and 100-fold. The empty vector pDEST22 was used as a negative control.

(B) Firefly luciferase complementation assays in tobacco leaves confirmed the interactions between TCPs and PIF4.

(C) Co-immunoprecipitation (coIP) indicated that PIF4 could be combined with TCP5 when both were transiently expressed in tobacco leaves.

(D) CoIP suggested that TCP13 and TCP17 could interact with PIF4 in tobacco leaves.

(E) CoIP with 35Spro-TCP5-FLAG 35Spro-PIF4-Myc transgenic plants confirmed the interaction between TCP5 and PIF4. Wild-type plants were used as negative controls.

(F) Analysis of PIF4 truncations suggested that the bHLH domain of PIF4 was responsible for the interaction with TCP5.

(G) Analysis of TCP5 truncations suggested that the TCP domain of TCP5 was required for the interaction with PIF4.

See also [Figure S2](#).

the petioles ([Figures 1I–1L](#)), consistent with the petiole elongation and reduced blade areas under HT. These observations further indicate that TCP5 acts as an important factor in the control of plant responses to HT.

### TCP5 Acts as a Transcriptional Activator

To determine the subcellular localization of TCP5, we generated TCP5pro-TCP5-GFP in which the *TCP5* promoter was used to drive the *TCP5-GFP* fusion gene. We observed clear green fluorescence in the nuclei of hypocotyl cells of TCP5pro-TCP5-GFP transgenic plants, consistent with the function of TCP5 as a transcription factor ([Figures S2A–S2D](#)). We then used a GAL4-UAS-LUC reporter system ([Guo et al., 2015](#); [Tao et al., 2013](#)) to test transactivation activity of TCPs. When the reporter was co-transformed with either GAL4DBD-PIF4 or GAL4DBD-TCP5, constructs in which the CaMV 35S promoter drives *PIF4* or *TCP5* fused to the sequence encoding the GAL4 DNA-binding domain (DBD), the *LUC* reporter gene was clearly activated, whereas in the negative controls, no fluorescence signal was observed ([Figure S2E](#)), indicating that TCP5 and PIF4 were transactivators. We further showed that the TCP domain was required for the transactivation activity of TCP5 because a truncated TCP5 with the TCP domain deleted could not activate the expression of reporter gene ([Figure S2F](#)). We also demonstrated that TCP13 and TCP17 were transactivators and that the TCP domain was required for their transactivation activity ([Figures S2G and S2H](#)).

### TCP5 Interacts with PIF4

To reveal the molecular mechanisms by which TCP5 controls plant thermomorphogenesis, we performed a yeast two-hybrid screen ([Ou et al., 2011](#)) using TCP5 as bait proteins and finally identified that PIF4 interacted with TCP5. We further confirmed this interaction by yeast two-hybrid assays, and results showed that TCP5, TCP13, and TCP17 all interacted with PIF4 fused with either the GAL4 activation domain or DBD ([Figure 2A](#)). Firefly luciferase complementation imaging indicated that TCP5, TCP13, and TCP17 indeed interacted with PIF4 ([Figure 2B](#)). We then confirmed the interaction of PIF4 with TCP5, TCP13, and TCP17 via co-immunoprecipitation (coIP) assays after transient expression in tobacco leaves ([Figures 2C and 2D](#)). We further used transgenic plants expressing PIF4-Myc and TCP5-FLAG to conduct coIP assays in planta, and the results indicated that TCP5 indeed interacted with PIF4 ([Figure 2E](#)). To identify the domains in TCP5 and PIF4 responsible for their interaction, we first deleted the C or N terminus, which includes the bHLH domain, of PIF4. The PIF4 deletions without the bHLH domain did not interact with TCP5 ([Figure 2F](#)). In addition, the bHLH domain of PIF4 was necessary and sufficient for the interaction between PIF4 and TCP5 ([Figure 2F](#)). We then made deletions of TCP5, and the results suggested that the TCP domain of TCP5 was required for its interaction with PIF4 ([Figure 2G](#)). These data suggested that TCP5 interacted with PIF4 and that their DBDs were necessary for TCP5-PIF4 interaction. To test whether TCP5 could also interact with PIF4 homologs including PIF1, PIF3, PIF5, and PIF7, which are key regulators in light signaling ([Leivar et al., 2008](#); [Leivar and Quail, 2011](#)), we carried out the yeast two-hybrid assays. The results showed that PIF1, PIF3, PIF5, and PIF7 all interacted with TCP5 ([Figure S2I](#)), suggesting that TCP5 might be also important for plant photomorphogenesis.

### TCP5 and PIF4 Regulates Common HT-Induced Genes

To identify the downstream targets of TCP5 and provide more evidence supporting the association of TCP5 with PIF4, we conducted RNA sequencing (RNA-seq) transcriptome analysis using petioles or blades from wild-type grown at normal temperatures (20°C), and wild-type, *tcp5tcp13tcp17* mutants, and *pif4* mutants treated with HT (28°C) for 6 h. We identified 1,081 differentially expressed genes (DEGs) (false discovery rate < 0.01; fold change  $\geq$  2.0 or  $\leq$  -2.0) (430 HT-induced genes and 651 HT-repressed genes) in petioles

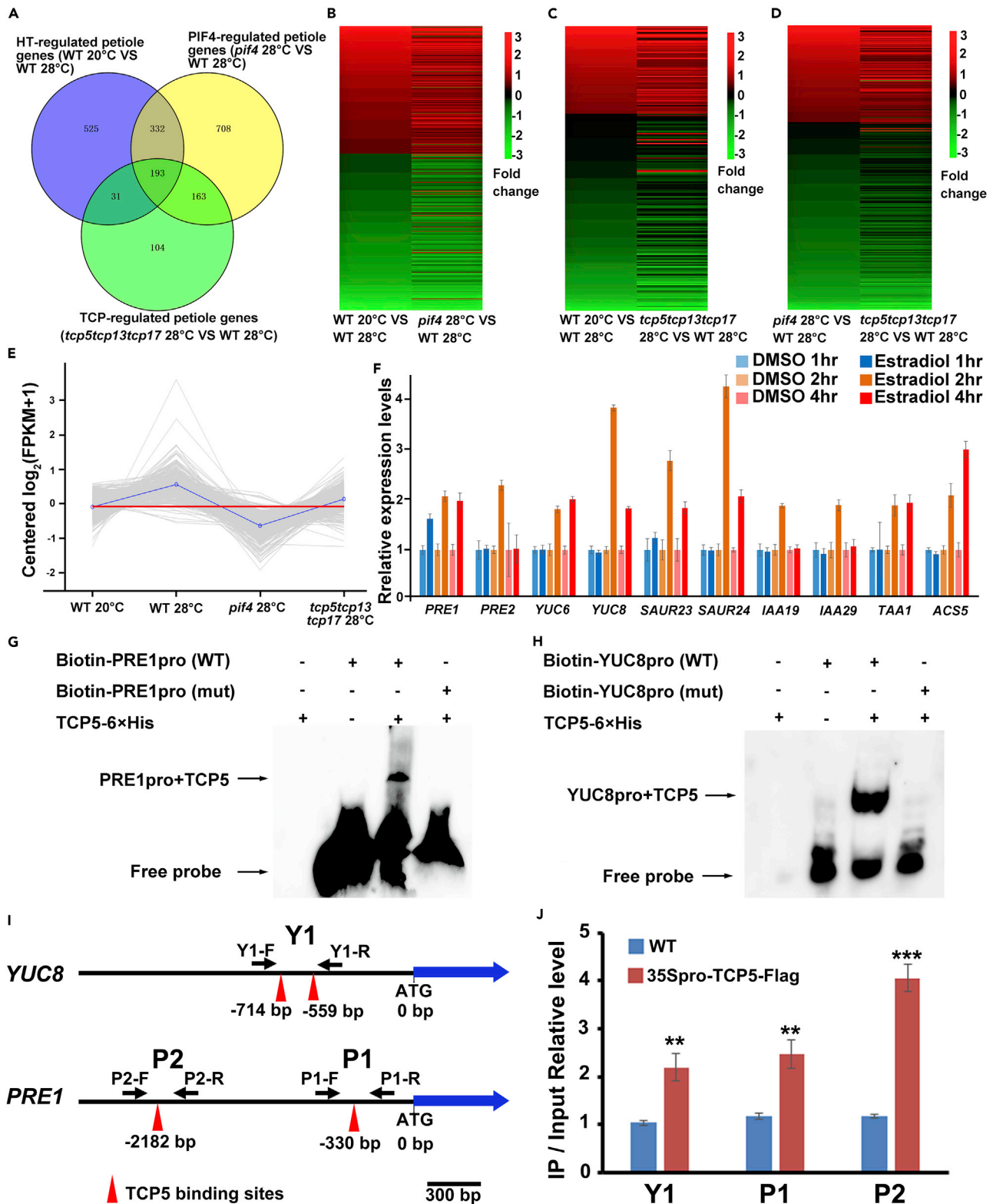


**Figure 3. TCP5 and PIF4 Co-regulate Common Target Genes**

(A) The Venn diagram indicates the numbers of differentially expressed genes (DEGs) coregulated by high temperature (HT), PIF4, and TCP5. (B) Heatmap of 525 DEGs coregulated by HT and PIF4.

**Figure 3. Continued**

(C) Heatmap of 224 DEGs coregulated by HT and TCPs.

(D) Heatmap of 356 DEGs coregulated by PIF4 and TCPs.

(E) Trend lines of 208 DEGs upregulated by HT and PIF4 suggested that most of these genes were also regulated by TCPs. The gray lines represent the relative expression of each gene. The blue line represents the mean relative expression of all genes.

(F) qRT-PCR analysis of known PIF4 direct target genes in TCP5-inducible pER8-iTCP5 transgenic plants. The pER8-iTCP5 transgenic plants were treated with 50  $\mu$ M estradiol or DMSO for 1, 2 or 4 h. The gene expression levels were normalized to that of *ACT8* and are relative to that in pER8-iTCP5 treated with DMSO. The data represent the mean  $\pm$  SD of three biological replicates.

(G) EMSA showed that TCP5 directly binds the promoter of *PRE1*.

(H) EMSA indicated that TCP5 directly binds the promoter of *YUC8*.

(I) Diagrams showing TCP5 binding motif in the promoter region of *YUC8* and *PRE1*. Y1-F/Y1-R, P1-F/P1-R, and P2-F/P2-R indicate PCR primer pairs used in (J).

(J) ChIP-PCR assays showed that TCP5 bound to the promoter region of *YUC8* and *PRE1*. 14-day-old wild-type (WT) and 35Spro-TCP5-FLAG plants grown under 20°C condition were collected for ChIP-PCR using the primer pairs as shown in (I). The data were first normalized to *ACT8* and then were relative to that of input DNA samples. The data represent mean  $\pm$  SD of three biological replicates.

See also [Figure S3](#), [Table S1](#), [S2](#), and [S3](#).

([Table S1](#)) after HT treatment. By contrast, only 558 DEGs (240 HT-induced genes and 318 HT-repressed genes) were found in the blades ([Table S1](#)), suggesting that the genes in the blade were less affected than those of the petiole by HT treatment. Furthermore, less than 13% (76/594) of HT-induced genes and approximately 20% (163/806) of HT-repressed genes were shared between the petioles and blades ([Figures S3A](#) and [S3B](#)). Interestingly, heatmaps of 594 HT-induced genes and 806 HT-repressed genes in leaves showed that the difference in the expression pattern of most genes in petioles was opposite in blades ([Figures S3C](#) and [S3D](#)). It is known that sessile plants display differential organ growth for adaptation in response to environmental cues. For example, light has opposite effects on the growth of cotyledons and hypocotyls. HT even differentially regulates the growth of two parts of one organ by promoting leaf petiole elongation and inhibiting the expansion of leaf blades. Recently, it has been shown that light differentially controls the expression of a class of *Small Auxin Up RNA (SAUR)* genes, which are responsible for the differential growth of cotyledons and hypocotyls under light ([Sun et al., 2016](#)). Our transcriptome data revealed that a large amount of genes were differentially expressed in leaf blades and leaf petioles after HT treatment ([Figures S3C](#) and [S3D](#)). These genes might also be very important for the opposite effects of HT on the growth of the two parts of leaves under HT.

As the transcriptomic changes in petioles were more obvious than those in blades, we then focused on comparing the petiole transcriptomes of *tcp5 tcp13 tcp17* or *pif4* mutants with those of wild-type under HT (28°C). Among the 1,396 PIF4-regulated petiole genes (DEGs between *pif4* mutants and wild-type under 28°C) ([Table S2](#)), more than 37% (525/1,396) of the genes were shared with HT-regulated genes (DEGs from wild-type with HT treatment) ([Figure 3A](#)), whereas almost 45% (224/491) of TCP-regulated petiole genes (DEGs between *tcp5 tcp13 tcp17* mutant and wild-type under 28°C) ([Table S2](#)) were included in HT-regulated genes ([Figure 3A](#)), suggesting that both PIF4 and TCPs played important roles in thermomorphogenesis. Interestingly, approximately 72% (356/491) of TCP-regulated genes were also regulated by PIF4 in petioles ([Figure 3A](#)). Gene Ontology analysis of these genes regulated by both TCPs and PIF4 showed that the pathway genes responding to abiotic or external and hormonal or internal stimuli were significantly enriched in the upregulated genes, whereas the cold pathway genes were enriched in the downregulated genes ([Figures S3E](#) and [S3F](#)), consistent with the important roles of PIF4 and TCPs in plant response to HT. Moreover, heatmap analysis showed that most of these coregulated genes were regulated in the same direction by HT and PIF4 ([Figure 3B](#)), HT and TCP ([Figure 3C](#)), or TCP and PIF4 ([Figure 3D](#)). These data provide strong evidence for the association of TCPs with PIF4 during thermomorphogenesis.

**TCP5 and PIF4 Shares Direct Target Genes including *PRE1* and *YUC8***

To find the direct target genes of TCP5, we first analyzed whether the downstream genes of PIF4 and HT could also be regulated by TCPs. Among 525 genes coregulated by HT and PIF4, 208 genes were upregulated. We retrieved the expression data for these 208 genes in petioles from RNA-seq data ([Table S3](#)). H-cluster (hierarchical cluster) analysis showed that the expression levels of most genes in *tcp5 tcp13 tcp17* mutants under HT were lower than those in wild-type under HT but higher than those in *pif4* mutants under HT ([Figure 3E](#)), implying that TCPs could enhance PIF4 activity. These 208 genes include many PIF4 direct target genes, such as *PRE1* ([Bai et al., 2012](#); [Oh et al., 2012](#)), *IAA19* ([Sun et al., 2013](#)), and *YUC8* ([Sun et al., 2012](#)) ([Figure S3G](#)). We further used qRT-PCR to test the changes in the expression of known PIF4

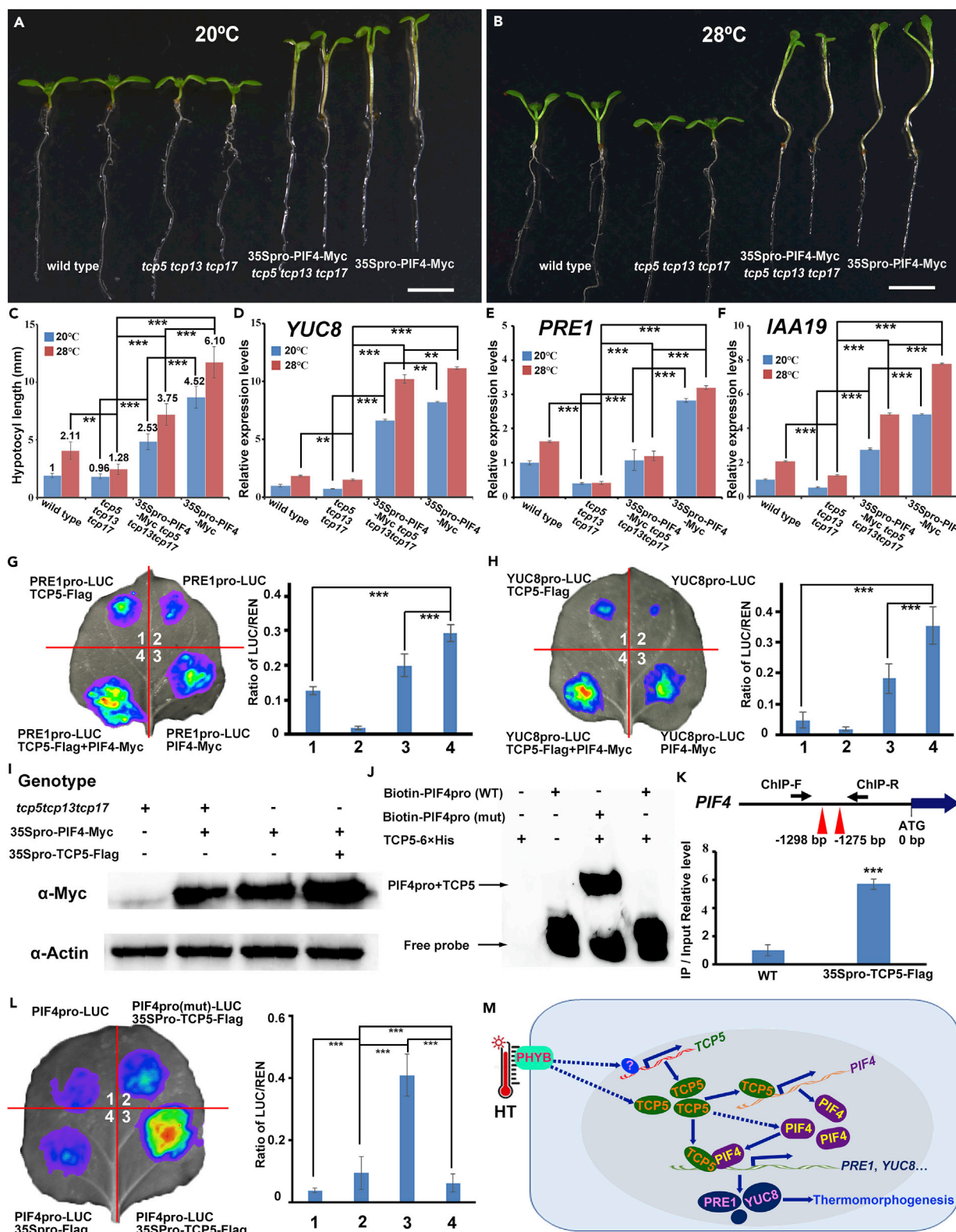


#### Figure 4. TCP5 Regulates PIF4 Activity at Both the Transcriptional and Post-transcriptional Levels

(A and B) The overexpression of PIF4 rescued the aberrant hypocotyl elongation of the *tcp5tcp13tcp17* triple mutant after HT treatment.

(C) The hypocotyl length of wild-type, *tcp5 tcp13 tcp17*, 35Spro-PIF4-Myc/*tcp5 tcp13 tcp17*, and 35Spro-PIF4-Myc under 20°C and 28°C. Data represent the mean  $\pm$  SD of three biological replicates,  $n > 20$ . Significant differences are indicated with \*\* $p < 0.01$  and \*\*\* $p < 0.001$ . The number above each column indicates fold changes of hypocotyl length relative to wild-type control under 20°C.

(D–F) qRT-PCR assays indicated the transcripts of (D) *YUC8*, (E) *PRE1*, and (F) *IAA19* in plants from (A) and (B). Seven-day-old seedlings grown under 20°C and then transferred to 20°C or 28°C for 2 h before harvesting total RNAs. Data represent the mean  $\pm$  SD of three biological replicates. Significant differences are indicated with \*\* $p < 0.01$  and \*\*\* $p < 0.001$ .

(G) Transient dual-luciferase expression in tobacco leaves showed that TCP5, with PIF4, strengthened the activation of *PRE1*.

(H) Transient dual-luciferase expression analysis in tobacco leaves indicated that TCP5, with PIF4, strengthened the activation of *YUC8*.

(I) The abundance of PIF4 protein in the *tcp5 tcp13 tcp17*, wild-type, or 35Spro-TCP5-FLAG backgrounds. Actin was used as an internal control. This experiment was repeated three times.

(J) EMSA showed that TCP5 directly bound the promoter of *PIF4* gene.

(K) ChIP-PCR assays showed that TCP5 bound to the promoter region of *PIF4*. 14-day-old wild-type and 35Spro-TCP5-FLAG plants grown under 20°C were collected for ChIP-PCR using the primer pairs as presented in top panel. The data were first normalized to *ACT8* and then were relative to that in input DNA samples. The data represent the mean  $\pm$  SD of three biological replicates.

(L) Transient expression assays demonstrated that TCP5 directly regulated the *PIF4*. The activity of REN was used as an internal control for normalization. The fluorescence ratio of LUC/REN represents the mean  $\pm$  SD of five biological replicates. Significant differences are indicated with \*\*\* $p < 0.001$  in (G), (H) and (L).

(M) A working model of TCPs in the regulation of thermomorphogenesis. HT induces *TCP5* transcription and stabilizes TCP5. The TCP5 that accumulates under HT can directly promote *PIF4* transcription and stabilize PIF4 protein. Moreover, TCP5 enhances PIF4 transactivation activity by interacting with PIF4. Many elongation- and auxin-related genes, such as *YUC8* and *PRE1*, were activated to promote hypocotyl and petiole elongation during thermomorphogenesis.

Scale bars, 5 mm in (A and B). See also [Figure S4](#).

direct target genes in wild-type, *pif4* mutant, and *tcp5 tcp13 tcp17* mutant after HT treatment. The results of qRT-PCR showed that the expression levels of *YUC8*, *PRE1*, and *IAA19* were rapidly upregulated in the petioles and hypocotyls of wild-type plants but were not or less induced in those of *pif4* mutant and *tcp5 tcp13 tcp17* mutant after HT treatment ([Figures S3H and S3I](#)). Moreover, we generated pER8-iTCP5 estrogen-inducible transgenic plants, and we found that pER8-iTCP5 plants produced longer hypocotyls after estrogen treatment ([Figures S3J and S3K](#)). We then briefly treated pER8-iTCP5 with estrogen in a time course (1, 2, or 4 h) to clarify downstream targets of TCP5. The qRT-PCR results showed that PIF4 direct target genes, including *PRE1* and *YUC8*, were rapidly upregulated by TCP5 ([Figure 3F](#)), suggesting that these genes might be direct targets of TCP5. We further used electrophoretic mobility shift assays (EMSAs) ([Figures 3G and 3H](#)) and chromatin immunoprecipitation quantitative polymerase chain reaction (ChIP-qPCR) ([Figures 3I and 3J](#)) to confirm that TCP5 protein could directly bind to the promoter of *YUC8* and *PRE1*. These direct target genes of both TCP5 and PIF4 support the idea that TCP5 controls plant thermomorphogenesis by associating with PIF4.

#### TCP5 Controls Plant Thermomorphogenesis by Regulating PIF4 at Transcriptional and Post-transcriptional Levels

To further support the interaction between TCP5 and PIF4, we conducted genetic analyses. We crossed 35Spro-PIF4-Myc with *tcp5 tcp13 tcp17* mutants and 35Spro-TCP5-FLAG with *pif4* mutants. The overexpression of *PIF4* rescued the short hypocotyl of *tcp5 tcp13 tcp17* mutants after HT treatment, whereas the long hypocotyls of the 35Spro-PIF4-Myc were partially rescued by the loss of TCP function in *tcp5 tcp13 tcp17* ([Figures 4A–4C](#)). However, we did not observe that the overexpression of *TCP5* could rescue the defects of *pif4* in response to HT ([Figures S4A–S4E](#)). We then tested the expression level of *YUC8*, *PRE1*, and *IAA19* coregulated by TCPs and PIF4 in these genetic materials. As predicted, the expression of these genes were downregulated in *tcp5 tcp13 tcp17*, but were upregulated in the overexpression lines of *PIF4* under HT or normal temperature ([Figures 4D–4F](#)). These data demonstrate that TCPs and PIF4 synergistically regulate plant thermomorphogenic growth.

To decipher the possible molecular mechanisms by which TCPs promote the function of PIF4, we first tested, based on the data in [Figures 3E and 3F](#), whether TCP5 could enhance the activity of PIF4. We cloned the promoters of *YUC8* and *PRE1*, which are direct target genes coregulated by TCP5 and PIF4. The promoters were used to drive the *LUC* reporter gene in PRE1pro-LUC and YUC8pro-LUC constructs. Transient expression assays in tobacco leaves suggested that the coexpression of PRE1pro-LUC or YUC8pro-LUC with either TCP5 or PIF4 could activate the *LUC* reporter, consistent with the observation that *PRE1* and *YUC8* are direct targets of both TCP5 and PIF4. We then coexpressed PRE1pro-LUC or YUC8pro-LUC with both TCP5 and PIF4, and the expression levels of *LUC* further drastically increased ([Figures 4G](#)

and 4H), suggesting that TCP5 and PIF4 act together to strengthen the activation of their coregulated genes. We then investigated whether TCP5 could prevent the degradation of PIF4 protein. We crossed the 35Spro-PIF4-Myc plants with 35Spro-TCP5-FLAG plants and *tcp5 tcp13 tcp17* mutant. We tested the abundance of PIF4-Myc protein and found that PIF4-Myc largely accumulated in 35Spro-TCP5-FLAG plant, but showed low abundance in the *tcp5 tcp13 tcp17* mutants (Figure 4I), suggesting that TCPs may have protected the PIF4 protein from degradation. In addition to the promotion of PIF4 stability by TCP5, the expression level of *PIF4* was strongly downregulated in *tcp5 tcp13 tcp17* under HT in our RNA-seq data (Figure S4F). Using qRT-PCR, we confirmed that *PIF4* was indeed highly repressed in *tcp5 tcp13 tcp17* under HT (Figure S4G). To test whether TCP5 might directly regulate *PIF4* gene, we used estradiol to treat pER8-iTCP5 transgenic plants and found that *PIF4* transcripts rapidly increased (Figure S4H). We searched the promoter of *PIF4* and found two possible TCP-binding sites. EMSA analysis and ChIP-qPCR indicated that the two binding sites were required for the direct binding of TCP5 to the promoter of *PIF4*, whereas mutations in the binding site disrupted TCP5 binding to the *PIF4* promoter in EMSA (Figures 4J and 4K). We further used the *PIF4* promoter or a *PIF4*-mutated promoter to drive the *LUC* reporter in PIF4pro-LUC or PIF4pro(mut)-LUC. Transient expression assays confirmed that TCP5 could directly bind to the promoter of *PIF4* so that *PIF4* expression could be activated (Figure 4L). These data suggest that TCP5 promotes the activity of PIF4 at both transcriptional and post-translation levels.

In this study, we demonstrate that TCP5 acts as an important component in the control of plant thermomorphogenesis by boosting PIF4 activity. We showed that *TCP5* is rapidly induced by HT and that HT stabilizes *TCP5* proteins. The overexpression of *TCP5* causes constitutive thermomorphogenesis under normal growth temperature, whereas thermomorphogenesis is compromised in the *tcp5 tcp13 tcp17* triple mutant. We propose a working model for the regulation of plant thermomorphogenesis by TCP5 (Figure 4M). HT promotes the transcription of *TCP5* and the stability of *TCP5* protein. On the one hand, *TCP5* directly binds the *PIF4* promoter and upregulates the transcriptional level of *PIF4*; on the other hand, *TCP5* directly interacts with PIF4 to promote the stability and activity of PIF4 protein. *TCP5* and PIF4 coactivate many HT-inducible genes to stimulate the growth of hypocotyls and petioles. Our data demonstrate that *TCP5* acts as a positive regulator of plant response to HT. TCPs control the biosynthesis of multiple plant hormones (Barkoulas et al., 2007; Challa et al., 2016; Danisman, 2016; Gonzalez-Grandio et al., 2017; Guo et al., 2010; Lopez et al., 2015; Nicolas and Cubas, 2016; Schommer et al., 2008; Steiner et al., 2012; Wang et al., 2015), including auxin (Challa et al., 2016; Koyama et al., 2010), BRs (Guo et al., 2010), jasmonic acid (Schommer et al., 2008), salicylic acid (Wang et al., 2015), and abscisic acid (Gonzalez-Grandio et al., 2017). Our findings suggest that TCPs might function as important relays that convert environmental cues such as HT into endogenous signals during plant morphological response to ever-changing environments.

### Limitations of the Study

In this study, we find that a clade of TCP transcription factors that include *TCP5*, *TCP13*, and *TCP17* act as important positive regulators by boosting PIF4 activity at both transcriptional and protein levels during thermomorphogenesis. Although this study provides a mechanism for fine-tuning PIF4 activity during plant responses to HT, the relationships between TCPs and other PIF4 interactors including BZR1 and phyB are still unknown. The coordination of TCPs with other numerous regulators in the tight control of PIF4 activity and plant thermomorphogenesis needs to be subsequently studied in future.

### METHODS

All methods can be found in the accompanying [Transparent Methods supplemental file](#).

### SUPPLEMENTAL INFORMATION

Supplemental Information can be found online at <https://doi.org/10.1016/j.isci.2019.04.005>.

### ACKNOWLEDGMENTS

We thank Prof. Li-Jia Qu and Prof. Hongya Gu (Peking University) for discussions and valuable suggestions. We thank Prof. Yuval Eshed (Weizmann Institute of Science, Israel) for kindly providing the *tcp5 tcp13 tcp17* triple mutant seeds and Prof. Hongwei Guo (Southern University of Science and Technology) for the *pif4* mutant seeds. This work was supported by the National Key Research and Development Program of China

(2017YFA0503800), the Science Fund for the Creative Research Groups of the National Natural Science Foundation of China (grant no. 31621001), and the National Science Fund for Distinguished Young Scholars of China (grant no. 31725005).

## AUTHOR CONTRIBUTIONS

X.H. and G.Q. designed all experiments, analyzed the data and wrote the manuscript. X.H. performed most of the experiments and collected the data. H.Y. generated the estradiol-inducible *TCP5* construct and pER8-iTCP5 transgenic plants. H.Y., R.Y., Y.Y., and F.A. contributed to the generation of transgenic plants and the analyses of phenotypes and RNA-seq data.

## DECLARATION OF INTERESTS

The authors declare no competing interests.

Received: November 13, 2018

Revised: March 5, 2019

Accepted: April 1, 2019

Published: May 8, 2019

## REFERENCES

- Aggarwal, P., Das Gupta, M., Joseph, A.P., Chatterjee, N., Srinivasan, N., and Nath, U. (2010). Identification of specific DNA binding residues in the TCP family of transcription factors in *Arabidopsis*. *Plant Cell* 22, 1174–1189.
- Aguilar-Martinez, J.A., Poza-Carrion, C., and Cubas, P. (2007). *Arabidopsis* BRANCHED1 acts as an integrator of branching signals within axillary buds. *Plant Cell* 19, 458–472.
- Bai, M.Y., Fan, M., Oh, E., and Wang, Z.Y. (2012). A triple helix-loop-helix/basic helix-loop-helix cascade controls cell elongation downstream of multiple hormonal and environmental signaling pathways in *Arabidopsis*. *Plant Cell* 24, 4917–4929.
- Barkoulas, M., Galinha, C., Grigg, S.P., and Tsiantis, M. (2007). From genes to shape: regulatory interactions in leaf development. *Curr. Opin. Plant Biol.* 10, 660–666.
- Bernardo-Garcia, S., de Lucas, M., Martinez, C., Espinosa-Ruiz, A., Daviere, J.M., and Prat, S. (2014). BR-dependent phosphorylation modulates PIF4 transcriptional activity and shapes diurnal hypocotyl growth. *Gene Dev.* 28, 1681–1694.
- Box, M.S., Huang, B.E., Domijan, M., Jaeger, K.E., Khattak, A.K., Yoo, S.J., Sedivy, E.L., Jones, D.M., Hearn, T.J., Webb, A.A., et al. (2015). ELF3 controls thermoresponsive growth in *Arabidopsis*. *Curr. Biol.* 25, 194–199.
- Challa, K.R., Aggarwal, P., and Nath, U. (2016). Activation of *YUCCA5* by the transcription factor TCP4 integrates developmental and environmental signals to promote hypocotyl elongation in *Arabidopsis*. *Plant Cell* 28, 2117–2130.
- Danisman, S. (2016). TCP transcription factors at the interface between environmental challenges and the plant's growth responses. *Front. Plant Sci.* 7, 1930.
- Delker, C., Sonntag, L., James, G.V., Janitza, P., Ibanez, C., Ziermann, H., Peterson, T., Denk, K., Mull, S., Ziegler, J., et al. (2014). The DET1-COP1-HY5 pathway constitutes a multipurpose signaling module regulating plant photomorphogenesis and thermomorphogenesis. *Cell Rep.* 9, 1983–1989.
- Efroni, I., Blum, E., Goldshmidt, A., and Eshed, Y. (2008). A protracted and dynamic maturation schedule underlies *Arabidopsis* leaf development. *Plant Cell* 20, 2293–2306.
- Foreman, J., Johansson, H., Hornitschek, P., Josse, E.M., Fankhauser, C., and Halliday, K.J. (2011). Light receptor action is critical for maintaining plant biomass at warm ambient temperatures. *Plant J.* 65, 441–452.
- Franklin, K.A., Lee, S.H., Patel, D., Kumar, S.V., Spartz, A.K., Gu, C., Ye, S., Yu, P., Breen, G., Cohen, J.D., et al. (2011). Phytochrome-interacting factor 4 (PIF4) regulates auxin biosynthesis at high temperature. *Proc. Natl. Acad. Sci. U S A* 108, 20231–20235.
- Gangappa, S.N., and Kumar, S.V. (2017). DET1 and HY5 control PIF4-mediated thermosensory elongation growth through distinct mechanisms. *Cell Rep.* 18, 344–351.
- Gonzalez-Grandio, E., Pajoro, A., Franco-Zorrilla, J.M., Tarancon, C., Immink, R.G., and Cubas, P. (2017). Abscisic acid signaling is controlled by a BRANCHED1/HD-ZIP 1 cascade in *Arabidopsis* axillary buds. *Proc. Natl. Acad. Sci. U S A* 114, E245–E254.
- Gonzalez-Grandio, E., Poza-Carrion, C., Sorzano, C.O., and Cubas, P. (2013). BRANCHED1 promotes axillary bud dormancy in response to shade in *Arabidopsis*. *Plant Cell* 25, 834–850.
- Guo, D., Zhang, J., Wang, X., Han, X., Wei, B., Wang, J., Li, B., Yu, H., Huang, Q., Gu, H., et al. (2015). The WRKY transcription factor WRKY71/EXB1 controls shoot branching by transcriptionally regulating RAX Genes in *Arabidopsis*. *Plant Cell* 27, 3112–3127.
- Guo, Z., Fujioka, S., Blancaflor, E.B., Miao, S., Gou, X., and Li, J. (2010). TCP1 modulates brassinosteroid biosynthesis by regulating the expression of the key biosynthetic gene *DWARF4* in *Arabidopsis thaliana*. *Plant Cell* 22, 1161–1173.
- Ibanez, C., Delker, C., Martinez, C., Burstenbinder, K., Janitza, P., Lippmann, R., Ludwig, W., Sun, H., James, G.V., Klecker, M., et al. (2018). Brassinosteroids dominate hormonal regulation of plant thermomorphogenesis via BZR1. *Curr. Biol.* 28, 303–310.e3.
- Jung, J.H., Domijan, M., Klose, C., Biswas, S., Ezer, D., Gao, M.J., Khattak, A.K., Box, M.S., Charoensawan, V., Cortijo, S., et al. (2016). Phytochromes function as thermosensors in *Arabidopsis*. *Science* 354, 886–889.
- Kieffer, M., Master, V., Waites, R., and Davies, B. (2011). TCP14 and TCP15 affect internode length and leaf shape in *Arabidopsis*. *Plant J.* 68, 147–158.
- Koini, M.A., Alvey, L., Allen, T., Tilley, C.A., Harberd, N.P., Whitelam, G.C., and Franklin, K.A. (2009). High temperature-mediated adaptations in plant architecture require the bHLH transcription factor PIF4. *Curr. Biol.* 19, 408–413.
- Koyama, T., Furutani, M., Tasaka, M., and Ohme-Takagi, M. (2007). TCP transcription factors control the morphology of shoot lateral organs via negative regulation of the expression of boundary-specific genes in *Arabidopsis*. *Plant Cell* 19, 473–484.
- Koyama, T., Mitsuda, N., Seki, M., Shinozaki, K., and Ohme-Takagi, M. (2010). TCP transcription factors regulate the activities of ASYMMETRIC LEAVES1 and miR164, as well as the auxin response, during differentiation of leaves in *Arabidopsis*. *Plant Cell* 22, 3574–3588.
- Legris, M., Klose, C., Burgie, E.S., Rojas, C.C., Neme, M., Hiltbrunner, A., Wigge, P.A., Schafer, E., Vierstra, R.D., and Casal, J.J. (2016). Phytochrome B integrates light and temperature signals in *Arabidopsis*. *Science* 354, 897–900.
- Leivar, P., Monte, E., Al-Sady, B., Carle, C., Storer, A., Alonso, J.M., Ecker, J.R., and Quail, P.H.

- (2008). The Arabidopsis phytochrome-interacting factor PIF7, together with PIF3 and PIF4, regulates responses to prolonged red light by modulating phyB levels. *Plant Cell* 20, 337–352.
- Leivar, P., and Quail, P.H. (2011). PIFs: pivotal components in a cellular signaling hub. *Trends Plant Sci.* 16, 19–28.
- Lopez, J.A., Sun, Y., Blair, P.B., and Mukhtar, M.S. (2015). TCP three-way handshake: linking developmental processes with plant immunity. *Trends Plant Sci.* 20, 238–245.
- Ma, D., Li, X., Guo, Y., Chu, J., Fang, S., Yan, C., Noel, J.P., and Liu, H. (2016). Cryptochrome 1 interacts with PIF4 to regulate high temperature-mediated hypocotyl elongation in response to blue light. *Proc. Natl. Acad. Sci. U S A* 113, 224–229.
- Martín-Trillo, M., and Cubas, P. (2010). TCP genes: a family snapshot ten years later. *Trends Plant Sci.* 15, 31–39.
- Nath, U., Crawford, B.C.W., Carpenter, R., and Coen, E. (2003). Genetic control of surface curvature. *Science* 299, 1404–1407.
- Nicolas, M., and Cubas, P. (2016). TCP factors: new kids on the signaling block. *Curr. Opin. Plant Biol.* 33, 33–41.
- Nieto, C., Lopez-Salmeron, V., Daviere, J.M., and Prat, S. (2015). ELF3-PIF4 interaction regulates plant growth independently of the evening complex. *Curr. Biol.* 25, 187–193.
- Nusinow, D.A., Helfer, A., Hamilton, E.E., King, J.J., Imaizumi, T., Schultz, T.F., Farre, E.M., and Kay, S.A. (2011). The ELF4-ELF3-LUX complex links the circadian clock to diurnal control of hypocotyl growth. *Nature* 475, 398–402.
- Oh, E., Zhu, J.Y., Bai, M.Y., Arenhart, R.A., Sun, Y., and Wang, Z.Y. (2014). Cell elongation is regulated through a central circuit of interacting transcription factors in the Arabidopsis hypocotyl. *Elife* 3, e03031.
- Oh, E., Zhu, J.Y., and Wang, Z.Y. (2012). Interaction between BZR1 and PIF4 integrates brassinosteroid and environmental responses. *Nat. Cell Biol.* 14, 802–809.
- Ou, B., Yin, K.Q., Liu, S.N., Yang, Y., Gu, T., Wing Hui, J.M., Zhang, L., Miao, J., Kondou, Y., Matsui, M., et al. (2011). A high-throughput screening system for Arabidopsis transcription factors and its application to Med25-dependent transcriptional regulation. *Mol. Plant* 4, 546–555.
- Palatnik, J.F., Allen, E., Wu, X., Schommer, C., Schwab, R., Carrington, J.C., and Weigel, D. (2003). Control of leaf morphogenesis by microRNAs. *Nature* 425, 257–263.
- Quint, M., Delker, C., Franklin, K.A., Wigge, P.A., Halliday, K.J., and van Zanten, M. (2016). Molecular and genetic control of plant thermomorphogenesis. *Nat. Plant* 2, 15190.
- Schommer, C., Palatnik, J.F., Aggarwal, P., Chételat, A., Cubas, P., Farmer, E.E., Nath, U., and Weigel, D. (2008). Control of jasmonate biosynthesis and senescence by miR319 targets. *PLoS Biol.* 6, e230.
- Somers, D.E., Sharrock, R.A., Tepperman, J.M., and Quail, P.H. (1991). The *hy3* long hypocotyl mutant of Arabidopsis is deficient in Phytochrome B. *Plant Cell* 3, 1263–1274.
- Song, J., Liu, Q., Hu, B., and Wu, W. (2017). Photoreceptor PhyB involved in Arabidopsis temperature perception and heat-tolerance formation. *Int. J. Mol. Sci.* 18, E1194.
- Stavang, J.A., Gallego-Bartolome, J., Gomez, M.D., Yoshida, S., Asami, T., Olsen, J.E., Garcia-Martinez, J.L., Alabadi, D., and Blazquez, M.A. (2009). Hormonal regulation of temperature-induced growth in Arabidopsis. *Plant J.* 60, 589–601.
- Steiner, E., Yanai, O., Efroni, I., Ori, N., Eshed, Y., and Weiss, D. (2012). Class I TCPs modulate cytokinin-induced branching and meristematic activity in tomato. *Plant Signal. Behav.* 7, 807–810.
- Sun, J., Qi, L., Li, Y., Zhai, Q., and Li, C. (2013). PIF4 and PIF5 transcription factors link blue light and auxin to regulate the phototropic response in Arabidopsis. *Plant Cell* 25, 2102–2114.
- Sun, J.Q., Qi, L.L., Li, Y.N., Chu, J.F., and Li, C.Y. (2012). PIF4-mediated activation of YUCCA8 expression integrates temperature into the auxin pathway in regulating Arabidopsis hypocotyl growth. *PLoS Genet.* 8, e1002594.
- Sun, N., Wang, J., Gao, Z., Dong, J., He, H., Terzaghi, W., Wei, N., Deng, X.W., and Chen, H. (2016). Arabidopsis SAURs are critical for differential light regulation of the development of various organs. *Proc. Natl. Acad. Sci. U S A* 113, 6071–6076.
- Tao, Q., Guo, D., Wei, B., Zhang, F., Pang, C., Jiang, H., Zhang, J., Wei, T., Gu, H., Ou, L.J., et al. (2013). The TIE1 transcriptional repressor links TCP transcription factors with TOPLESS/TOPLESS-RELATED corepressors and modulates leaf development in Arabidopsis. *Plant Cell* 25, 421–437.
- Tasset, C., Singh Yadav, A., Sureshkumar, S., Singh, R., van der Woude, L., Nekrasov, M., Tremethick, D., van Zanten, M., and Balasubramanian, S. (2018). POWERDRESS-mediated histone deacetylation is essential for thermomorphogenesis in Arabidopsis thaliana. *PLoS Genet.* 14, e1007280.
- Toledo-Ortiz, G., Johansson, H., Lee, K.P., Bou-Torrent, J., Stewart, K., Steel, G., Rodriguez-Concepcion, M., and Halliday, K.J. (2014). The HY5-PIF regulatory module coordinates light and temperature control of photosynthetic gene transcription. *PLoS Genet.* 10, e1004416.
- Wang, X., Gao, J., Zhu, Z., Dong, X., Wang, X., Ren, G., Zhou, X., and Kuai, B. (2015). TCP transcription factors are critical for the coordinated regulation of isochlorismate synthase 1 expression in Arabidopsis thaliana. *Plant J.* 82, 151–162.
- Wei, B., Zhang, J., Pang, C., Yu, H., Guo, D., Jiang, H., Ding, M., Chen, Z., Tao, Q., Gu, H., et al. (2015). The molecular mechanism of sporocytless/nozzle in controlling Arabidopsis ovule development. *Cell Res.* 25, 121–134.
- Wigge, P.A. (2013). Ambient temperature signalling in plants. *Curr. Opin. Plant Biol.* 16, 661–666.
- Yang, Y., Nicolas, M., Zhang, J., Yu, H., Guo, D., Yuan, R., Zhang, T., Yang, J., Cubas, P., and Qin, G. (2018). The TIE1 transcriptional repressor controls shoot branching by directly repressing BRANCHED1 in Arabidopsis. *PLoS Genet.* 14, e1007296.
- Zhang, B., Holmlund, M., Lorrain, S., Norberg, M., Bako, L., Fankhauser, C., and Nilsson, O. (2017). BLADE-ON-PETIOLE proteins act in an E3 ubiquitin ligase complex to regulate PHYTOCHROME INTERACTING FACTOR 4 abundance. *Elife* 6, e26759.
- Zhang, X., Ji, Y., Xue, C., Ma, H., Xi, Y., Huang, P., Wang, H., An, F., Li, B., Wang, Y., et al. (2018). Integrated regulation of apical hook development by transcriptional coupling of EIN3/EIL1 and PIFs in Arabidopsis. *Plant Cell* 30, 1971–1988.

ISCI, Volume 15

**Supplemental Information**

***Arabidopsis* Transcription Factor TCP5**

**Controls Plant Thermomorphogenesis**

**by Positively Regulating PIF4 Activity**

**Xiang Han, Hao Yu, Rongrong Yuan, Yan Yang, Fengying An, and Genji Qin**

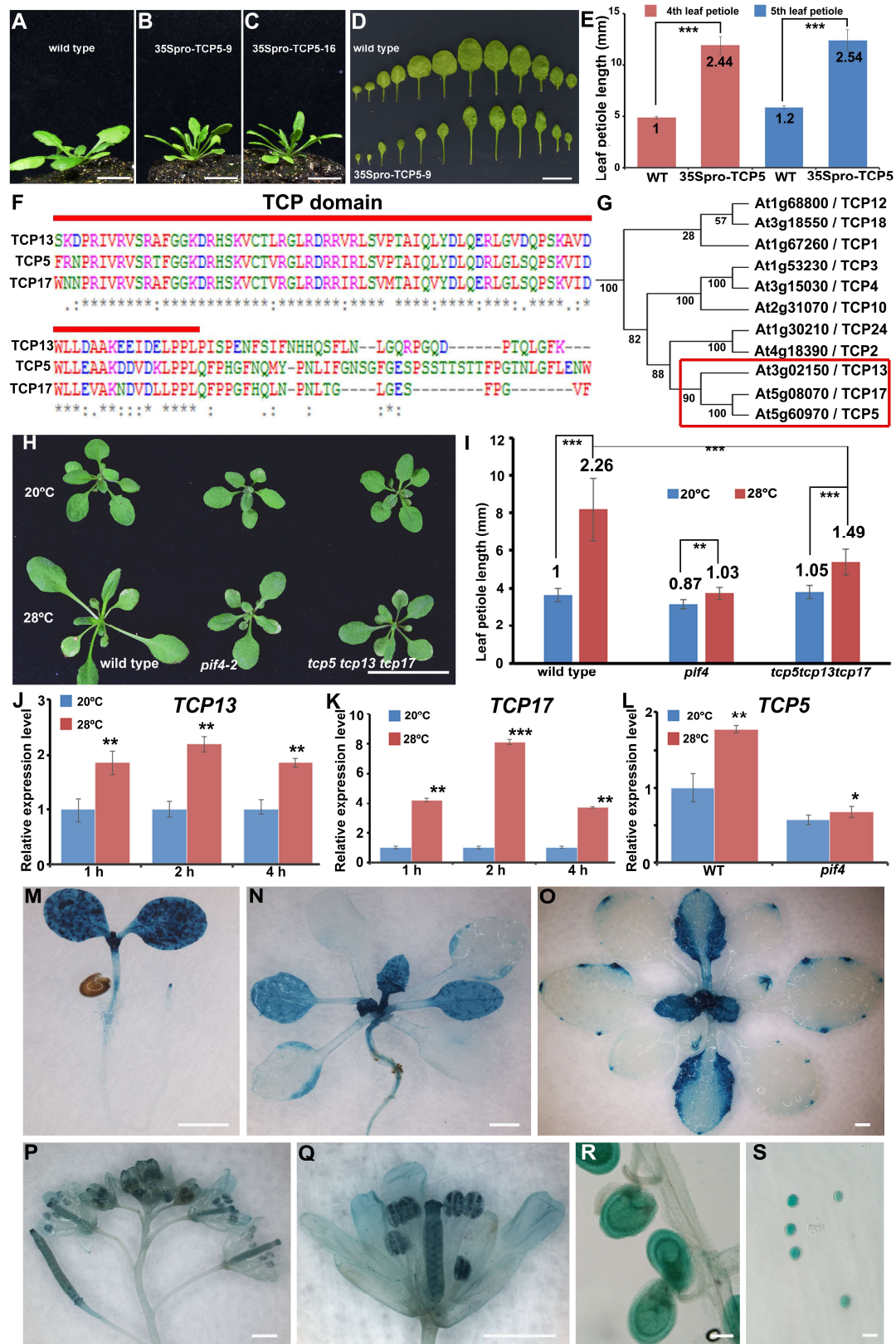
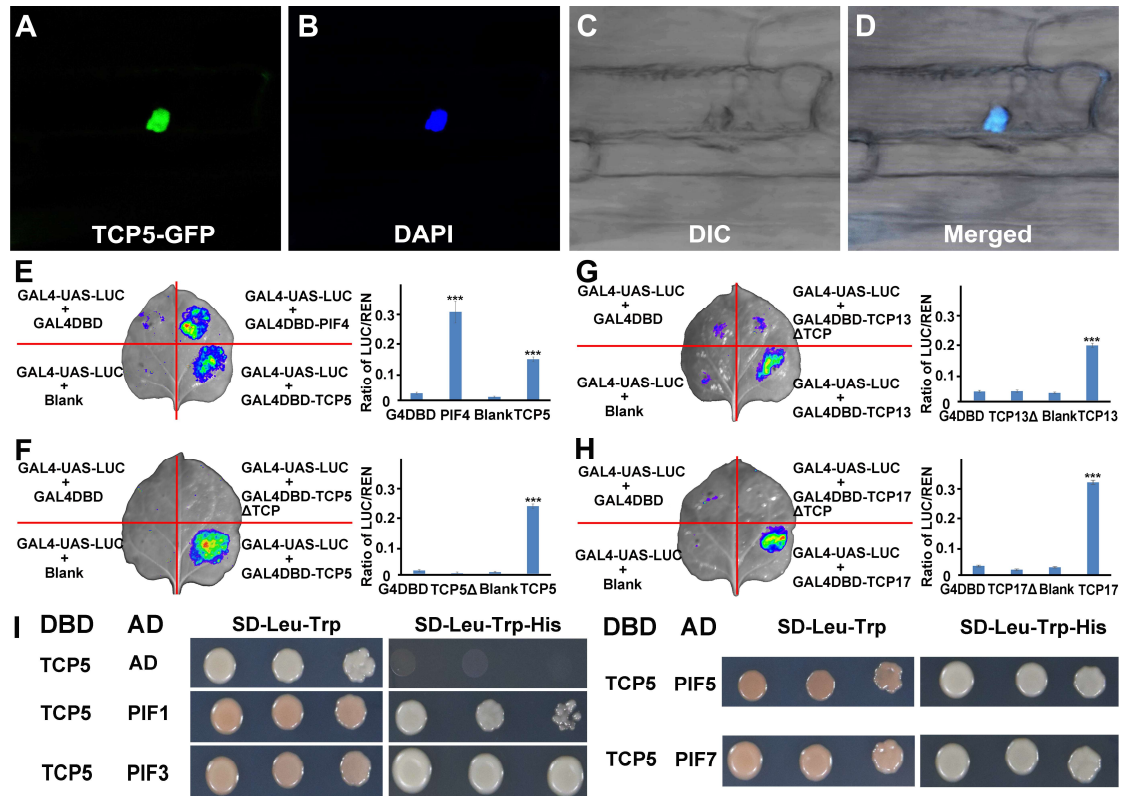


Figure S1. TCP5 and its close homologs participate in plant thermomorphogenesis, Related to Figure 1.

(A-C) 21-day-old wild-type (A), 35Spro-TCP5-Flag-9 (B) and 35S-TCP5-FLAG-16 (C) plants. The leaves grow upward in 35Spro-TCP5-Flag at 20°C. (D) Dissected leaves of 21-day-old wild-type and 35Spro-TCP5-Flag-9 plants at 20°C. (E) Quantitative analysis of length of the 4th and 5th petioles from wild type and 35Spro-TCP5-Flag-9. Significant differences are indicated with \*\*\* ( $P < 0.01$ ,  $n > 20$ , two-tailed Student's t-test). The number above each column means fold changes of petiole length relative to wild type. (F) Protein alignment assays showing that TCP5, TCP13 and TCP17 share a conserved noncanonical bHLH domain. (G) Phylogenetic analysis of the full lengths of the class II TCP family in Arabidopsis. TCP5, TCP13 and TCP17 are grouped in a small subclade, suggesting that they have high similarity. The phylogenetic tree was constructed using MEGA 6.0 with default settings. (H) 26-day-old wild type, *pif4* mutant and *tcp5tcp13tcp17* mutant. 21-day-old plants grown in continuous 20°C before transferring to 20°C or 28°C for 5 additional days of growth. (I) Quantitative analysis of the length of the 5th petiole of wild type, *pif4* mutant and *tcp5tcp13tcp17* mutant. The data represent the mean  $\pm$  SD of three biological replicates. Significant differences are indicated with \* ( $P < 0.05$ ,  $n > 20$ ) and \*\*\* ( $P < 0.001$ ). The number above each column means fold changes of hypocotyl length relative to that of wild type under 20°C. (J) and (K) Relative expression levels of *TCP13* (J) and *TCP17* (K) in wild type after HT treatment for 1, 2 or 4 hours. The expression levels were normalized to that of *ACT8* and were relative to that of wild-type control under 20°C. Data represent the mean  $\pm$  SD of three biological replicates. (L) The expression changes of TCP5 in *pif4* mutant under 20°C or 28°C. (M) GUS staining of 10-day-old TCP5pro-GUS transgenic seedlings. (N) GUS staining of 21-day-old TCP5pro-GUS transgenic plants. (O) GUS staining of 28-day-old TCP5pro-GUS transgenic plants. (P) GUS staining of inflorescence from 35-day-old TCP5pro-GUS transgenic plants. (Q) GUS staining of flowers from 35-day-old TCP5pro-GUS transgenic plants. (R) GUS staining of ovules from 35-day-old TCP5pro-GUS transgenic plants. (S) GUS staining of pollen grains from 35-day-old TCP5pro-GUS transgenic plants. Scale bars, 1 cm in (A-C), 1.5 mm in (D), 2 cm in (H), 1 mm in (M-Q), 50  $\mu$ m in (R) and (S).



**Figure S2. The subcellular localization of TCP5 and the transactivation activity of TCP5, TCP13 and TCP17, Related to Figure 2.**

(A) Green fluorescence detected in the hypocotyls of TCP5pro-TCP5-GFP seedlings. (B) Nuclei stained with DAPI. (C) Bright field image of TCP5pro-TCP5-GFP hypocotyl. (D) Image merge of DAPI and GFP. (E) PIF4 and TCP5 act as transactivators. (F-H) TCP5, TCP13 and TCP17 work as transactivators, and their transactivation activity is dependent on the bHLH domains of TCP5 (F), TCP13 (G) and TCP17 (H). (I) Yeast two hybrid assays showed that TCP5 interacted with PIF1, PIF3, PIF5 and PIF7. Co-transformed yeast cells were grown on medium lacking Leu and Trp (SD-Leu-Trp) and selected on medium lacking Leu, Trp and His (SD-Leu-Trp-His) with or without 10 mM 3-AT at dilutions of 10 and 100 fold. The empty vector pDEST22 was used as a negative control. Scale bars, 10  $\mu$ m in (A-D).

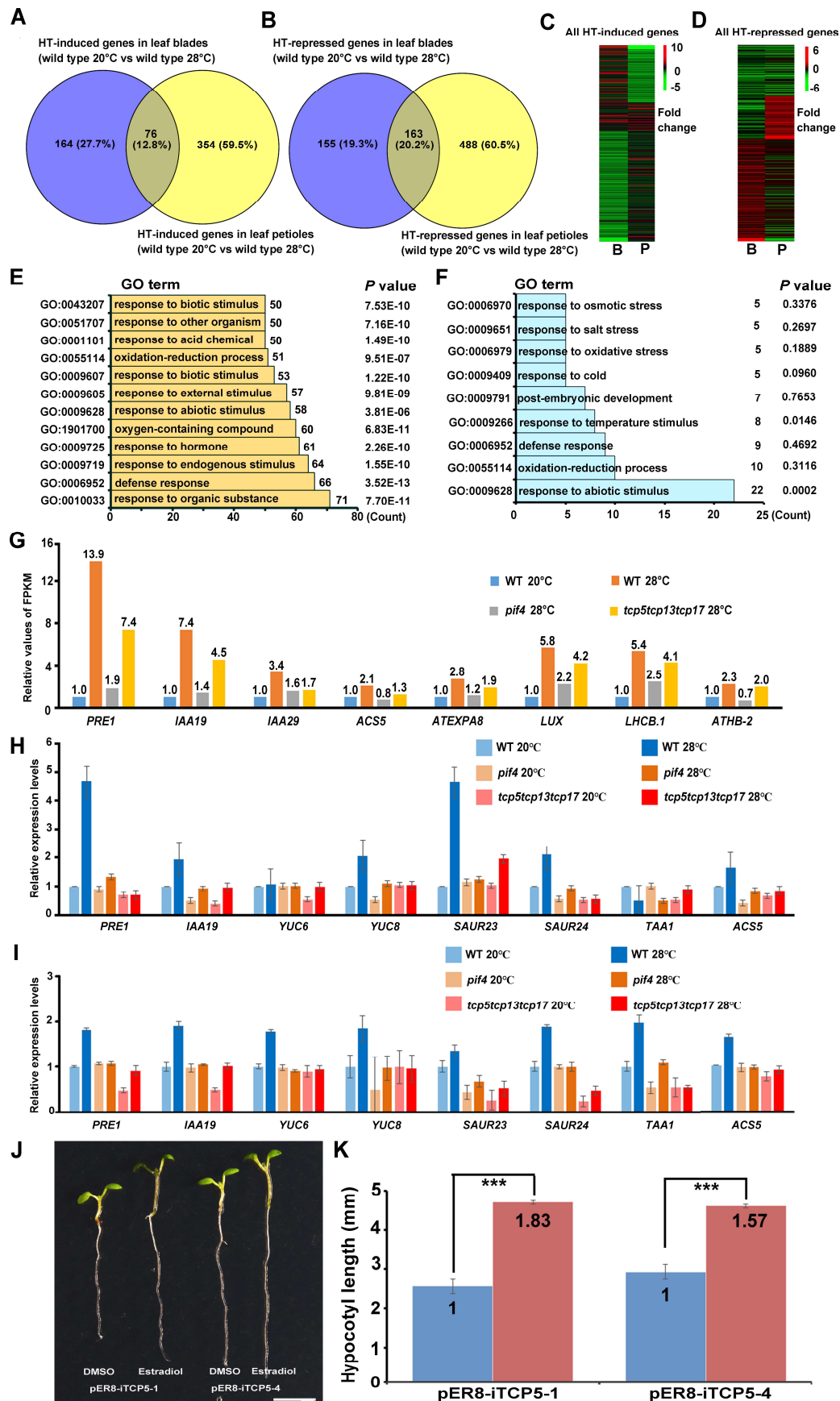
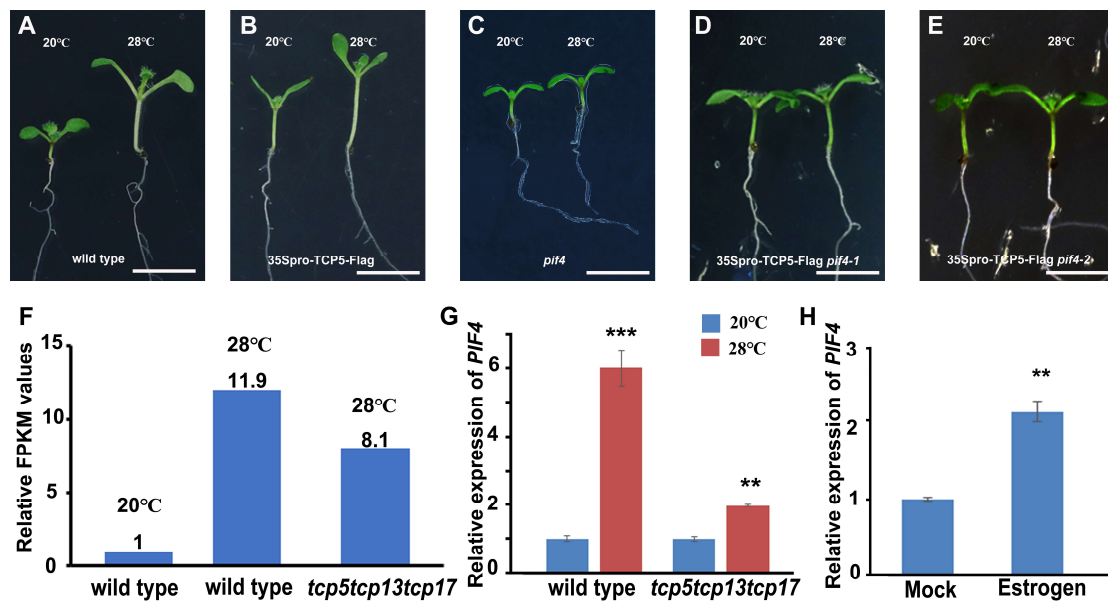


Figure S3. Transcriptomes regulated by HT in petioles and leaf blades, and the target genes regulated by TCPs, Related to Figure 3.

(A) Venn diagrams of genes upregulated by HT in petioles and leaf blades. (B) Venn diagrams of genes downregulated by HT in petioles and leaf blades. (C) Heat map of genes upregulated by HT in petioles and leaf blades. (D) Heat map of genes downregulated by HT in petioles and leaf blades. Scale bars indicate the fold changes of the DEGs. (E) GO analysis of genes up-regulated by both PIF4 and TCPs in petioles. (F) GO analysis of down-regulated by both PIF4 and TCPs in petioles. GO analysis were performed by DIVID 6.8 with default settings. (G) Diagrams of relative FPKM values of PIF4 direct target genes from RNA-seq data in WT at 20°C and 28°C, *pif4* at 28°C and *tcp5tcp13tcp17* at 28°C. (H) qRT-PCR analysis of the expression levels of TCPs- and PIF4-coregulated genes from hypocotyls. 7-day-old wild-type, *pif4* mutant and *tcp5tcp13tcp17* mutant seedlings grown under continuous 20°C before transferring to 28°C for additional 2 hours. *ACT8* was used as an internal control. (I) qRT-PCR analysis of the expression levels of TCPs- and PIF4-coregulated genes from petioles. 21-day-old, *pif4* and *tcp5tcp13tcp17* mutant grown in continuous 20°C before transferring to 28°C for additional 2 hours. *ACT8* was used as an internal control. (J) Estradiol- or mock-induced pER8-iTCP5-1 and pER8-iTCP5-4 transgenic plants. 10-day-old seedlings which were first grown for 3 days and then treated with 50  $\mu$ M estradiol or DMSO for 7 days under 20°C. (K) Quantitative analysis of the hypocotyl lengths of pER8-iTCP5-1 and pER8-iTCP5-4 in (J). These data represent the mean  $\pm$  SD of three biological replicates. Significant differences are indicated with \*\*\* (P < 0.001, n>20). The number above each column means fold changes of hypocotyl length relative to mock treatment. Scale bar=5 mm in (J).



**Figure S4. Genetic and regulation analysis between TCP5 and PIF4. Related to Figure 4.**

(A-E) Overexpression of *TCP5* could not rescue the insensitivity of *pif4* mutant in response to HT. The hypocotyl of wild type (A), *pif4* (B), 35Spro-TCP5-Flag (C) and 35Spro-TCP5-Flag *pif4-1* (D) and 35Spro-TCP5-Flag *pif4-2* (E) under 20°C and 28°C. (F) Diagrams of relative FPKM values of *PIF4* gene from RNA-seq data in wild type at 20°C, wild type treated with 28°C, *tcp5tcp13tcp17* treated with 28°C. (G) qRT-PCR analysis of the expression level of *PIF4* gene from hypocotyls. 7-day-old wild-type and *tcp5tcp13tcp17* seedlings grown under continuous 20°C before transferring to 28°C for 2 additional hours. *ACT8* was used as an internal control. The data represent the mean  $\pm$  SD of three biological replicates. (H) qRT-PCR analysis of *PIF4* in TCP5-inducible pER8-iTCP5 transgenic plants. The pER8-iTCP5 transgenic plants were treated with 50  $\mu$ M estradiol or DMSO for 2 hours. The gene expression levels were normalized to that of *ACT8* and are relative to that in pER8-iTCP5 treated with DMSO. The data represent the mean  $\pm$  SD of three biological replicates.

**Table S4. The list of oligonucleotides used in this study. Related to Figure 1, 2, 3 and 4.**

| <b>Oligonucleotide name</b>                  | <b>sequence (5' - 3')</b>                    |
|--|--|
| <b>Oligonucleotides for constructs</b>       |  |
| PIF4-F                                       | CACCATGGAACACCAAGTTGG                        |
| PIF4-R-NSC                                   | TCCGTGGTCCAAACGAGAACCGTC                     |
| PIF4-R-SC                                    | CTATCCGTGGTCCAAACGAGAACCGTC                  |
| TCP5-F                                       | CACCATGAGATCAGGAGAATGTGATGAAGAG              |
| TCP5-R-NSC                                   | AGAATCTGATTCATTATCGC                         |
| TCP5-R-SC                                    | TCAAGAATCTGATTCATTATCGC                      |
| TCP5-F1                                      | CCGCTCGAGATGAGATCAGGAGAATGTGA                |
| TCP5-R1                                      | GGACTAGTTCAAGAATCTGATTCATTAT                 |
| TCP13-F                                      | CACCATGAATATCGTCTCTTGAAAGATGC                |
| TCP13-R-NSC                                  | CATATGGTGATCACTTCCTCTA                       |
| TCP13-R-SC                                   | TCACATATGGTGATCACTTCCTCTA                    |
| TCP17-F                                      | CACCATGGGAATAAAAAAGAAGATCA                   |
| TCP17-R-NSC                                  | CTCGATATGGTCTGGTTGTGAG                       |
| TCP17-R-SC                                   | CTACTCGATATGGTCTGGTTGTGAG                    |
| TCP5pro-F1                                   | CACCTGCCAAATCCTGTCATACATTCCCAA               |
| TCP5pro-R1                                   | CTCTTTAATCACTCAACAAGATCTTCA                  |
| TCP5pro-F2                                   | GGGACAACCTTTGTATAGAAAAGTTGCTGCCAAATCCTGTCATA |
| TCP5pro-R2                                   | GGGACTGCTTTTTTGTACAACTTGCTCTTTAATCACTCAAC    |
| YUC8pro-F                                    | GGGACAACCTTTGTATAGAAAAGTTGCTAAAGTGTCTAGATGA  |
| YUC8pro-R                                    | GGGACTGCTTTTTTGTACAACTTGCTAAGTTTCTTTAATAAGT  |
| PRE1pro-F                                    | GGGACAACCTTTGTATAGAAAAGTTGCTTCATGCCAACCTGTCG |
| PRE1pro-R                                    | GGGACTGCTTTTTTGTACAACTTGCCATGTTCAACAATGTGG   |
| PIF4pro(wt)-F                                | GGGACAACCTTTGTATAGAAAAGTTGCTACACCATCACGAATTT |
| PIF4pro(wt)-R                                | GGGACTGCTTTTTTGTACAACTTGCTAGCGTTATGTTTTTGT   |
| PIF4pro(mut)-F                               | GGATATGGGTGATTACAAGTAGGCACAATGGGTGACTAAT     |
| PIF4pro(mut)-R                               | ATTAGTACCCATTGTGCCTACTTGTAATCACCCATATCC      |
| <b>Oligonucleotides for yeast two hybrid</b> |  |
| PIF4 $\Delta$ N53-F                          | CACCATGGATCATCATGAAGAAGCCCTAAGAT             |
| PIF4 $\Delta$ C-R                            | TTAATGAACTTCAGCTGCTCGACTCCTT                 |
| PIF4 $\Delta$ N-F                            | CACCATGATGTGGATGGGAGTGGAATGGCG               |
| PIF4-bHLH-F                                  | CACCATGAATCTCTCCGAAAGGAGGAGG                 |
| PIF4-bHLH-R                                  | TTACTTGAAGCTGTAAGTGAAGTGA                    |
| TCP5 $\Delta$ N1-F                           | CACCATGCCTCCTCTACAATCCCACATGGATTTAAC         |
| TCP5 $\Delta$ TCP-R                          | GAATGTTCTTGAGACTCGAACGATTCTTGATTC            |
| TCP5 $\Delta$ TCP-F                          | GAATCCAAGAATCGTTCGAGTCTCAAGAACATTC           |
| TCP5 $\Delta$ N2-F                           | CACCATGGGTGGCAAAGACAGACACAGCAAAG             |
| <b>Oligonucleotides for genotyping</b>       |  |

|                                     |                                  |
|-------------------------------------|----------------------------------|
| TCP5-SM-LP                          | TGAATCTGTTTTCTCCATCC             |
| TCP5-SM-RP                          | CTCGAAGCAGCAAAGATGAC             |
| TCP13-SM-LP                         | TTCCTGTTCAAGCTCAAGACC            |
| TCP13-SM-RP                         | GACCGACGACATCCGATTATC            |
| TCP17-SALK-LP                       | TCTTTGGATCCTCAGATCTTCC           |
| TCP17-SALK-RP                       | ATGTACCTTTGCTCGCATCAG            |
| PIF4-SALK-LP                        | AATTCATCATCGGGGATTAGG            |
| PIF4-SALK-RP                        | TCGTCGTTTAATAAACACGGC            |
| SM-P                                | TACGAATAAGAGCGTCCATTTTAGAGTGA    |
| SALK-P                              | ATTTTGCCGATTTTCGGAAC             |
| <b>Oligonucleotides for qRT-PCR</b> |                                  |
| ACTIN8-qRT-F                        | TGTGCCAATCTACGAGGGTTT            |
| ACTIN8-qRT-R                        | TTTCCCGCTCTGCTGTTGT              |
| PIF4-qRT-F                          | CCAGATCATCTCCGACCGGTTTG          |
| PIF4-qRT-R                          | CTAGTGGTCCAAACGAGAACCGT          |
| YUC6-qRT-F                          | TGGCAGCTCAAGACTTATGACCGT         |
| YUC6-qRT-R                          | TCCGGCTTTATGTCAAACCTCCGA         |
| YUC8-qRT-F                          | TGTATGCGGTTGGGTTTACGAGGA         |
| YUC8-qRT-R                          | CCTTGAGCGTTTCGTGGGTTGTTT         |
| PRE1-qRT-F                          | GTTCTGATAAGGCATCAGCCTCG          |
| PRE1-qRT-R                          | CATGAGTAGGCTTCTAATAACGG          |
| PRE2-qRT-F                          | CCGTCGTTCCAACACGGTATCA           |
| PRE2-qRT-R                          | CTGCGGCTTGTGGGCTATTAGG           |
| IAA19-qRT-F                         | GGTGACAACCTGCGAATACGTTACCA       |
| IAA19-qRT-R                         | CCCGGTAGCATCCGATCTTTTCA          |
| IAA29-qRT-F                         | CACGGCGATGAACAACAACATAT          |
| IAA29-qRT-R                         | CTCTGTCGCAATCTTCATATTTCG         |
| ACS5-qRT-F                          | GCGATGCTTTCCTTTTGCCTACTC         |
| ACS5-qRT-R                          | TTTCTGGGCTTGTGGTAAGCTTGT         |
| SAUR23-qRT-F                        | ATTCAAACTTTCAGACAAAAGAAATGG      |
| SAUR23-qRT-R                        | ACAAGGAAACAACCTCTATCTCTAACT      |
| SAUR24-qRT-F                        | GAGATATTTGGTGCCTGTCTCATATTTAAACC |
| SAUR24-qRT-R                        | CAAGAAGAAAGAGGAAAAAGGGCTCATC     |
| TAA1-qRT-F                          | CCCTGCGTTTTCGTGGCTAGGGA          |
| TAA1-qRT-R                          | GAGCTTCATGTTGGCGAGTCTCT          |
| TCP5-qRT-F                          | GGGTTTAACACCAATCATCAACAA         |
| TCP5-qRT-R                          | CGACAGTAACGTTATTACCAGATT         |
| TCP13-qRT-F                         | CTGGTTCAGGGACTATGGAGACATT        |
| TCP13-qRT-R                         | AAATGTTTTGGGAAGACGAAGATGA        |
| TCP17-qRT-F                         | GGTAACGTCACTGTCGCATTTTCTAA       |
| TCP17-qRT-R                         | GAAACGAAGGGTACCTTGTGGGA          |

| <b>Oligonucleotides for EMSA</b>     |  |
|--------------------------------------|--|
| TCP5-6*HIS-F                         | CACCTCTAGAATGATATTTAGGTGACACTATAGAACAGACCACC   |
| TCP5-6*HIS-R                         | CTCGAGAAAAAAAAAAAAAAAAAATTAATGGTGATGGTGATGA    |
| PIF4-EMSA-F(+3')                     | ATGGGATATGGTCCATTACAAGTAGGCACAATGGTCCACTAAT    |
| PIF4-EMSA-R                          | ATAACAATTATTAGTGGACCATTGTGCCTACTTGTAATGGACCA   |
| PIF4-EMSA-mut-F(+3')                 | ATGGGATATGGGTGATTACAAGTAGGCACAATGGGTGACTAAT    |
| PIF4-EMSA-mut-R                      | ATAACAATTATTAGTCACCCATTGTGCCTACTTGTAATCACCCA   |
| YUC8-EMSA-F(+3')                     | TCTTCCCACGTGGCTTCCTCTCGTTGGTCCACAAAGAAT        |
| YUC8-EMSA-R                          | ATTCTTTGTGGGACCAACGAGAGGAAGCCACGTGGGGAAGA      |
| YUC8-EMSA-mut-                       | TCTTCCCACGTGGCTTCCTCTCGTTGGGTGCACAAAGAAT       |
| YUC8-EMSA-mut-R                      | ATTCTTTGTGCACCCAACGAGAGGAAGCCACGTGGGGAAGA      |
| PRE1-EMSA-F(+3')                     | ATGGTGGTGACACGTGACATAGTCGATGTTTTGTGAACATTTAT   |
| PRE1-EMSA-R                          | ATTGTTTCGATTGGTCCATTATTGGTTGAGTATTAATTTATATAAA |
| PRE1-EMSA-mut-                       | ATGGTGGTGACACGGGACATAGTCGATGTTTTGTGAACATTTAT   |
| PRE1-EMSA-mut-R                      | ATTGTTTCGATTGGGTGATTATTGGTTGAGTATTAATTTATATAA  |
| <b>Oligonucleotides for ChIP-PCR</b> |  |
| YUC8-Y1-F                            | ATGTGGAGATGGCGGGACCAAGAAA                      |
| YUC8-Y1-R                            | GGGTGATTCTTTGTGGGACCAACGA                      |
| PRE1-P1-F                            | CAGCATGTAACACGAGACATGGTGG                      |
| PRE1-P1-R                            | CGGCTTTAAACTTCGTTTCAGACCA                      |
| PRE1-P2-F                            | ACACAATAACTAACTAACCATGATTGAAAACG               |
| PRE1-P2-R                            | AATAAACCTCGACAATGATGTCACG                      |
| PIF4-ChIP-F                          | TGATATACATTTTCAGGAAAACCTTAGC                   |
| PIF4-ChIP-R                          | GGAAAAAGATCTAGTATGTTCTTCG                      |

## Transparent Methods.

### KEY RESOURCES TABLE

| REAGENT or RESOURCE  | SOURCE        | IDENTIFIER    |
|--|---------------|---------------|
| Antibodies   |               |               |
| Mouse anti-MYC antibody                                    | CMCTAG        | Cat. AT0023   |
| Mouse anti-FLAG antibody with HRP conjugating              | Sigma-Aldrich | Cat. A8592    |
| Mouse anti-plant actin antibody                            | Sigma-Aldrich | Cat. A0480    |
| EZview™ red anti-c-Myc affinity gel                        | Sigma-Aldrich | Cat. E6654    |
| Anti-FLAG® M2 Magnetic Beads                               | Sigma-Aldrich | Cat. M8823    |
| Goat anti-mouse HRP-conjugated IgG                         | CWBIO         | Cat. Cw0102   |
| Bacterial and Virus Strains                                |               |               |
| <i>E.coli</i> strain DH5 $\alpha$                          | N/A           | N/A           |
| <i>A. tumefaciens</i> GV3101                               | N/A           | N/A           |
| Yeast strain AH109   | N/A           | N/A           |
| Chemicals, Peptides, and Recombinant Proteins              |               |               |
| $\beta$ -Estradiol   | Sigma-Aldrich | Cat. E2758    |
| DAPI (4',6-diamidino-2-phenylindole dihydrochloride)       | VECTOR        | Cat. H-1200   |
| 3-AT (3-amino-1,2,4 triazole)                              | Sigma-Aldrich | Cat. A9126    |
| D-Luciferin  | Sigma-Aldrich | Cat. L0594    |
| X-gluc (5-Bromo-4-chloro-3-indolyl $\beta$ -D-glucuronide) | Sigma-Aldrich | Cat. B5285    |
| Critical Commercial Assays                                 |               |               |
| First-strand cDNA reverse transcription kit                | Promega       | Cat. A3500    |
| Dual-luciferase reporter kit                               | Promega       | Cat. E1910    |
| TNT SP6 high-yield wheat germ protein expression kit       | Promega       | Cat. L3260    |
| pENTR/D-TOPO Cloning Kit                                   | Thermo Fisher | Cat. K240020  |
| Gateway LR Clonase II Enzyme mix                           | Thermo Fisher | Cat. 11791020 |
| LightShift™ Chemiluminescent EMSA kit                      | Thermo Fisher | Cat. 20148    |
| Experimental Models: Organisms/Strains                     |               |               |
| Arabidopsis: WT Col-0                                      | N/A           | N/A           |
| Arabidopsis: <i>tcp5</i>                                   | [29]          | SM_3_29639    |
| Arabidopsis: <i>tcp13</i>                                  | [29]          | SM_3_23151    |
| Arabidopsis: <i>tcp17</i>                                  | [29]          | SALK_147288   |
| Arabidopsis: <i>pif4</i>                                   | [12]          | SALK_140393C  |
| 35Spro-PIF4-MYC/ <i>tcp5tcp13tcp17</i>                     | This study    | N/A           |
| 35Spro-TCP5-FLAG/ <i>pif4-1</i>                            | This study    | N/A           |

|                                  |                          |   |
|----------------------------------|--------------------------|---|
| 35Spro-TCP5-FLAG/ <i>pif4-2</i>  | This study               | N/A   |
| 35Spro-PIF4-MYC/35Spro-TCP5-FLAG | This study               | N/A   |
| Recombinant DNA                  |                          |   |
| TCP5pro-GUS                      | This study               | N/A   |
| TCP5pro-TCP5-GFP                 | This study               | N/A   |
| 35Spro-PIF4-Myc                  | This study               | N/A   |
| 35Spro-TCP5-Flag                 | This study               | N/A   |
| pER8-iTCP5                       | This study               | N/A   |
| 35Spro-TCP13-Flag                | This study               | N/A   |
| 35Spro-TCP17-Flag                | This study               | N/A   |
| PIF4pro-LUC                      | This study               | N/A   |
| PIF4mpro-LUC                     | This study               | N/A   |
| PRE1pro-LUC                      | This study               | N/A   |
| YUC8pro-LUC                      | This study               | N/A   |
| Software and Algorithms          |                          |   |
| ImageJ                           | N/A                      | <a href="https://imagej.net/">https://imagej.net/</a><br>Welcome          |
| Excel (2016)                     | Microsoft Office Excel   | N/A   |
| Photoshop (cc2018)               | Adobe                    | N/A   |
| MEGA (6.0)                       | N/A                      | <a href="https://www.megasoftware.net/">https://www.megasoftware.net/</a> |
| DIVID (6.8)                      | N/A                      | <a href="https://david.ncifcrf.gov/">https://david.ncifcrf.gov/</a>       |
| BMK Cloud                        | Biomarker Technology Co. | <a href="https://www.biocloud.net/">https://www.biocloud.net/</a>         |

## EXPERIMENTAL MODEL AND SUBJECT DETAILS

### Plant materials and growth conditions

The *Arabidopsis thaliana* ecotype Columbia-0 (Col-0) was used as the wild type in this study. T-DNA mutants and various transgenic plants were in the Col-0 background. The T-DNA insertion mutants were *tcp5*, *tcp13*, *tcp17* (Efroni et al., 2008) and *pif4* (Zhang et al., 2018). The transgenic plants are described below. Wild-type, mutant and transgenic seeds were first sterilized using 15% (v/v) sodium hypochlorite solution and then plated on half-strength Murashige and Skoog medium, which was supplemented with 20 µg/mL DL-phosphinothricin, 50 µg/mL kanamycin or 50 µg/mL hygromycin B if necessary. The seeds were then synchronized at 4°C for 3 days and then placed in a 20±1°C growth chamber with long-day (16-hour light and 8-hour dark) conditions for 7 days. Green seedlings were transferred to soil and put in a 20±1°C greenhouse or growth chamber under long-day conditions. *Nicotiana benthamiana* was grown in soil and put in the same greenhouse for transient expression assays. For high-temperature

treatment, 7-day-old seedlings or 21-day-old plants were transferred to a 28±1°C growth chamber for 3 days or 5 days.

### **Accession numbers**

Gene annotations and data in this article can be found in The Arabidopsis Information Resource (TAIR) database using the following accession numbers: TAIR: AT5G60970 (TCP5), TAIR: AT3G02150 (TCP13), TAIR: AT5G08070 (TCP17), TAIR: AT2G43010 (PIF4), TAIR: AT5G39860 (PRE1), and TAIR: AT4G28720 (YUCCA8).

## **METHOD DETAILS**

### **PCR analysis and gene expression assays**

All the primers used in this study are listed in Table S4.

The T-DNA insertion mutants were genotyped using the primers TCP5-SM-LP, TCP5-SM-RP and SM-P; TCP13-SM-LP, TCP13-SM-RP and SM-P; TCP17-SALK-LP, TCP17-SALK-RP and SALK-P; or PIF4-SALK-LP, PIF4-SALK-RP and SALK-P for *tcp5*, *tcp13*, *tcp17* and *pif4*, respectively. PCR was performed for 30 cycles (94°C for 20 s, 52-60°C for 20 s, and 72°C for 90 s).

To perform qRT-PCR, total RNA from seedlings, petioles or blades were extracted by TRIzol reagent (Invitrogen) and reverse-transcribed using reverse transcription kit (Promega) according to the manufacturer's instructions. The products were used as the templates for qRT-PCR, which was conducted in an Applied Biosystems 7500 Fast Real-time PCR system with UltraSYBR Mixture (CW BIO, CW2601) as described in the manual. The PCR conditions were 95°C for 10 min, then performed 40 cycles under conditions of 94°C for 10 s, 58-60°C for 15 s, and 72°C for 25 s. Each experiment was repeated three times. *ACT8* was used as an internal control. The relative expression levels were evaluated via the  $2^{-\Delta\Delta CT}$  (cycle threshold) method (Livak and Schmittgen, 2001).

### **Generation of binary constructs and transgenic plants**

To examine the expression pattern of *TCP5*, the 2400-bp promoter upstream of the *TCP5* start codon was amplified using primers TCP5pro-F1 and TCP5pro-R1 and then cloned into pENTR/D-TOPO (Invitrogen) to generate TCP5pro-TOPO. The TCP5pro-GUS vectors were generated via an LR reaction with TCP5pro-TOPO and pKGWFS7 (Ghent University).

To determine the subcellular localization of *TCP5*, the 2400-bp promoter upstream of the *TCP5* start codon was amplified using primers TCP5pro-F2 and TCP5pro-R2 and then cloned into pDONR-P4P1R (Invitrogen) to generate TCP5pro-P4P1R. And the coding region of *TCP5* without stop codon was amplified using primers TCP5-F and TCP5-R-NSC and then cloned into pENTR/D-TOPO (Invitrogen) to generate TCP5NSC-TOPO. The *GREEN FLUORESCENT PROTEIN (GFP)* gene was amplified

from pK7WGF2 (Ghent University) using primers GFP-F and GFP-R and then cloned into pDONR-P2R-P3 (Invitrogen) to generate GFP-P2RP3. TCP5pro-TCP5-GFP was generated via an LR reaction with TCP5pro-P4P1R, TCP5NSC-TOPO, GFP-P2RP3 and pK7m34GW (Ghent University).

To obtain the *PIF4* and *TCP5* overexpression lines, *PIF4* without stop codon was amplified with PIF4-F and PIF4-R-NSC and cloned into pENTR/D-TOPO to generate PIF4NSC-TOPO. The 35Spro-PIF4-Myc or 35Spro-TCP5-Flag constructs were generated via an LR reaction with PIF4NSC-TOPO and pK7MYCGW2 (Li et al., 2016) or with TCP5NSC-TOPO and pK7FLAGGW2 (Li et al., 2016).

To obtain estrogen-inducible *TCP5* transgenic plants, *TCP5* was amplified using primer TCP5-F1, which had an *Xho* I site, and primer TCP5-R1, carrying a *Spe* I site. The PCR products and pER8 vectors were digested by *Xho* I and *Spe* I. The pER8-*i*TCP5 vectors were generated by ligating *Xho* I-*Spe* I-digested PCR products with the *Xho* I-*Spe* I-digested pER8 vector.

To generate 35Spro-TCP13-Flag and 35Spro-TCP17-Flag, *TCP13* and *TCP17* were amplified using primers TCP13-F and TCP13-R-NSC and primers TCP17-F and TCP17-R-NSC, respectively. The two genes were cloned into pENTR/D-TOPO to generate TCP13NSC-TOPO and TCP17NSC-TOPO. The 35Spro-TCP13-Flag and 35Spro-TCP17-Flag constructs were generated via an LR reaction between TCP13NSC-TOPO or TCP17NSC-TOPO and pK7FLAGGW2.

To test TCP5 binding to the *PIF4* promoter, the *PIF4* promoter was amplified using primers PIF4pro(wt)-F and PIF4pro(wt)-R and then cloned into pDONR-P4P1R to generate PIF4pro-P4P1R. pENTR/D-FLUC was generated as described previously (Guo et al., 2015). The PIF4pro-LUC reporter was generated via LR reactions with PIF4pro-P4P1R, pENTR/D-FLUC and pH7m24GW (Ghent University). To generate the *PIF4* mutated promoter, mutations in the *cis*-element (5'-TGGTCC-3' mutated to 5'-TGGGTG-3') were included in primers PIF4pro(mut)-R and PIF4pro(mut)-F. PIF4pro(wt)-F and PIF4pro(mut)-R or PIF4pro(mut)-F and PIF4pro(wt)-R were used to amplify the two halves of the *PIF4* mutated promoter. The two halves were then mixed together and used as PCR templates with primers PIF4pro(wt)-F and PIF4pro(wt)-R to obtain the *PIF4* mutated promoter. The *PIF4* mutated promoter was cloned into pDONR-P4P1R to generate PIF4mpro-P4P1R. The PIF4mpro-LUC reporter was generated via an LR reaction with PIF4mpro-P4P1R, pENTR/D-FLUC and pH7m24GW.

To generate PRE1pro-LUC and YUC8pro-LUC, the *PRE1* and *YUC8* promoters were amplified using *PRE1*pro-F and *PRE1*pro-R or *YUC8*pro-F and *YUC8*pro-R. The fragments were cloned into pDONR-P4P1R to generate PRE1pro-P4P1R or YUC8pro-P4P1R. The PRE1pro-LUC and YUC8pro-LUC reporter vectors were generated via an LR reaction with PRE1pro-P4P1R or YUC8pro-P4P1R, pENTR/D-FLUC and pH7m24GW.

The binary constructs were transformed into *Agrobacterium* strain GV3101 by electroporation. Transgenic *Arabidopsis* were generated using the floral dip method.

For genetic analysis, 35Spro-PIF4-Myc *tcp5tcp13tcp17* was obtained by crossing 35Spro-PIF4-Myc with *tcp5tcp13tcp17*. The 35Spro-PIF4-Myc 35Spro-TCP5-Flag line was obtained by crossing 35Spro-PIF4-Myc with 35Spro-TCP5-Flag.

### **Staining and microscopy**

Tissues from TCP5pro-GUS lines were fixed in 90% acetone overnight at 4°C and then washed three times using 1× phosphate buffer (pH 6.0). The samples were then immersed into GUS staining buffer solution (1 mg/mL X-gluc in phosphate buffer) and placed under vacuum for 2 hours. The samples were kept in a 37°C incubator for 12~24 hours and then transferred into 75% ethanol to stop staining before observation.

To observe subcellular localization, 7-day-old TCP5pro-TCP5-GFP seedlings were treated with DAPI staining solution for 5-10 min and observed using a Leica TCS SPE confocal microscope. The GFP signal was observed at 488 nm, and the DAPI signal was observed at 340 nm.

### **The measurement of hypocotyl and petiole lengths**

Pictures of hypocotyls or petioles were first taken using a Canon digital camera, and their lengths were then measured using ImageJ software. To analyze hypocotyl elongation under HT, 7-day-old seedlings growing at 20°C were transferred to 28°C for further growing 3 days before being photographed. To analyze petiole elongation under HT, 21-day-old plants growing under 20°C were transferred to 28°C for further growing 5 days before being photographed. The experiments were repeated three times. The data were then analyzed using Microsoft Excel, and statistical significance was determined using Student's t test ( $n > 20$ ).

### **Yeast two-hybrid assays**

To test the PIF4 and TCPs interaction, prey constructs PIF4-AD or TCPs-AD were generated via LR reactions between PIF4-TOPO or TCPs-TOPO and pDEST22 (Invitrogen). To generate the bait constructs, a truncated PIF4 $\Delta$ 53 with the first 53 amino acids of the N-terminus deleted was used because full-length PIF4 can activate the reporter in yeasts. PIF4 $\Delta$ 53 was amplified from PIF4-TOPO plasmids using primers PIF4 $\Delta$ 53-F and PIF4-R-SC and cloned into pENTR/D-TOPO to generate PIF4 $\Delta$ 53-TOPO. The bait constructs DBD-PIF4 $\Delta$ 53 and DBD-TCPs were generated via an LR reaction between PIF4 $\Delta$ 53-TOPO or TCP-TOPO and pDEST32 (Invitrogen). Each bait construct was cotransformed with each prey construct or empty pDEST22 into yeast strain AH109 (Clontech).

To further determine the PIF4 region responsible for the interaction with TCP5, truncated *PIF4* fragments were amplified using primers PIF4-F and PIF4 $\Delta$ C-R, PIF4 $\Delta$ N-F and PIF4-R-SC or PIF4-bHLH-F and PIF4-bHLH-R and were then cloned

into pENTR/D-TOPO to generate PIF4 $\Delta$ C-TOPO, PIF4 $\Delta$ N-TOPO and PIF4-bHLH-TOPO. The prey constructs PIF4 $\Delta$ C-AD, PIF4 $\Delta$ N-AD and PIF4-bHLH-AD were generated via an LR reaction between PIF4 $\Delta$ C-TOPO, PIF4 $\Delta$ N-TOPO or PIF4-bHLH and pDEST22. The DBD-TCP5 vector was cotransformed with each prey construct or empty pDEST22 into yeast strain AH109. The bait DBD-TCP5 was cotransformed with each prey construct or empty pDEST22 into yeast strain AH109.

To determine the region in TCP5 responsible for the interaction with PIF4, truncated *TCP5* fragments were amplified using primers TCP5 $\Delta$ N1-F and TCP5-R, TCP5-F and TCP5 $\Delta$ TCP-R, TCP5 $\Delta$ TCP-F and TCP5-R, and TCP5 $\Delta$ N2-F and TCP5-R and were then cloned into pENTR/D-TOPO to generate TCP5 $\Delta$ N1-TOPO, TCP5 $\Delta$ TCP-TOPO and TCP5 $\Delta$ N2-TOPO. The bait constructs were generated via an LR reaction between pDEST32 and TCP5 $\Delta$ N1-TOPO, TCP5 $\Delta$ TCP-TOPO or TCP5 $\Delta$ N2-TOPO. Each bait construct was cotransformed with PIF4-AD or empty pDEST22 into yeast strain AH109.

The yeast was grown in a 30°C incubator for 3 days. Selection was conducted using SD-Leu-Trp-His (GeneStar) medium with or without 10 mM 3-AT.

### **Protein extraction and immunoblotting**

Plant tissues were ground in liquid nitrogen and then suspended in native buffer (50 mM Tris-MES, pH 8.0, 0.5 M sucrose, 1 mM MgCl<sub>2</sub>, 10 mM EDTA, 1 mM PMSF) with 5 mM DL-dithiothreitol (DTT) and 1×complete protease inhibitor. The mixtures were kept on ice for 30 min and then centrifuged at 13,000 rpm at 4°C for 15 min. The supernatant was combined with 5×loading buffer (60 mM Tris-HCl, 20% glycerol, 8% SDS, 0.5% Coomassie Brilliant Blue, 2% mercaptoethanol and 10 mM DTT) and then loaded onto 12% SDS/PAGE gels for electrophoresis.

To confirm the interaction between PIF4 and TCPs via co-immunoprecipitation assays, 35Spro-PIF4-Myc and 35Spro-TCPs-Flag were coinfiltrated into tobacco leaves for transient expression as described previously. Total protein from tobacco leaves or transgenic Arabidopsis transformed with both 35S-PIF4-Myc and 35S-TCP5-Flag was extracted and incubated with anti-Flag beads overnight. Anti-Myc or anti-Flag antibodies were used to detect TCP5-Flag or PIF4-Myc. The membranes were incubated in anti-Myc or anti-Actin antibodies diluted 5,000-fold in 3% milk. Anti-Flag antibody conjugated with HRP was diluted 10,000-fold and incubated with the membrane in 3% milk. The secondary goat anti-mouse HRP-conjugated IgG was diluted 5,000-fold. Stable peroxide solution and luminol/enhancer solution (Thermo Scientific, SJ257615) were used for HRP-based detection.

### **Firefly luciferase complementation imaging**

To test the PIF4 interaction with TCPs *in vivo*, PIF4-nLUC was generated via an LR reaction between PIF4-TOPO and pCB1300-nLUC-GW (Zhang et al., 2017). cLUC-

TCPs constructs were generated via an LR reaction between TCPs-TOPO and pCB1300-cLUC-GW (Zhang et al., 2017). PIF4-nLUC and cLUC-TCPs were transformed into *Agrobacterium* strain GV3101. Different combinations of plasmids were coinfiltrated into tobacco leaves. The plants were grown for 72 hours under long-day conditions. The tobacco leaves were sprayed with 100 mM D-luciferin and kept in the dark for 15 min. The fluorescence was detected using a low-light cooled charge-coupled device (CCD) imaging apparatus (NightOWL II LB983) with indiGO software.

### **Transient expression analysis in tobacco leaves**

The reporter constructs including PRE1pro-LUC, YUC8pro-LUC, PIF4pro-LUC, and PIF4mpro-LUC and the constructs 35Spro-TCP5-Flag and 35Spro-PIF4-Myc were as described above. The control construct, 35Spro-Flag, was generated via an LR reaction between 3Flag-TOPO and pB7FLAGGW2. The constructs were transformed into *Agrobacterium* strain GV3101. Each reporter was cotransformed into tobacco leaves with pCambia-1300-P19, 35Spro-REN (Guo et al., 2015; Zhang et al., 2017), 35Spro-TCP5-Flag and/or 35Spro-PIF4-Myc, or the control constructs. After incubation for 3 days, the tobacco leaves were treated with luciferin and observed using a CCD imaging apparatus. The firefly (*Photinus pyralis*) and Renilla (*Renilla reniformis*) luciferase activities were measured using dual-luciferase reporter kits with GloMax® 20/20 luminometer (Promega). The fluorescence intensity of REN was used as an internal control. At least three biological repeats were performed.

For dual-luciferase reporter assays of PIF4pro-LUC or PIF4mpro-LUC and TCP5, experimental groups combined with PIF4pro-LUC or PIF4mpro-LUC and 35Spro-3×Flag or PIF4pro-LUC and 35Spro-TCP5-Flag or PIF4mpro-LUC and 35Spro-TCP5-Flag were cotransformed with pCambia-1300-P19 and 35S-REN into tobacco leaves. After 3 days of incubation, the tobacco leaves were treated with luciferin and observed using a CCD imaging apparatus.

### **Electrophoretic mobility shift assay (EMSA)**

An 84-bp probe containing possible TCP binding motifs (5'-GGACCA-3') in the *PRE1* promoter and its corresponding control probe, in which only the motif (5'-GGACCA-3') was mutated to 5'-CACCCA-3', were synthesized and labeled with biotin at the 3'-end by a company (Invitrogen). A 41-bp probe containing possible TCP binding motifs (3'-GGACCA-5') in the *YUC8* promoter and its corresponding control probe, in which the motif was mutated to 3'-CAGCCA-5', were synthesized and labeled with biotin at the 3'-end. A 52-bp probe containing possible TCP binding motifs (5'-GGACCA-3') in the *PIF4* promoter and its corresponding control probe, in which the motif was mutated to 5'-CACCCA-3', were synthesized and labeled with biotin at the 3'-end. The TCP5-His protein was expressed using a TNT SP6 high-yield wheat germ protein expression system in vitro according to the manufacturer's instructions. The double-stranded

probes were acquired by annealing equimolar concentrations of both complementary oligoes in annealing buffer (10 mM Tris, pH 7.5, 1 mM EDTA, and 50 mM NaCl). EMSAs were performed using a LightShift™ Chemiluminescent EMSA kit according to the manual. Reaction mixtures containing TCP5 protein and probes were incubated at room temperature for 30 minutes, and the products were loaded onto 12% nondenaturing polyacrylamide gels.

### **RNA-seq analysis**

Wild type, *pif4* and *tcp5tcp13tcp17* plants were grown at 20°C for 3 weeks and then transferred to a 28°C growth chamber for 3 days. Total RNA was extracted from the petioles of wild type, *pif4* or *tcp5tcp13tcp17* plants treated with HT for 3 days and from the petioles of the control, which was the wild type continually grown under 20°C. RNA-seq was performed on a HiSeq Illumina Hisequation 2000 platform in the Biomedical Pioneering Innovation Center (BIOPIC) of Peking University. The clean reads were separated from random adapters and low-quality reads. The RNA-seq data were analyzed using a platform from Biomarker Technology Co. (Beijing, China, <https://www.biocloud.net/>). To find differentially expressed genes (DEGs), HISAT2 (<http://ccb.jhu.edu/software/hisat2/index.shtml>) was used to align the reads to the TAIR10 and StringTie (<https://ccb.jhu.edu/software/stringtie/index.shtml>) was used to normalize and calculate the FPKM (fragments per kilobase of exon per million fragments mapped) values as the expression value of each gene. To find the DEGs, RNA-seq data from two samples were analyzed using EBseq (R package version 1.20.0). The false discovery rate (FDR) < 0.01 and fold change  $\geq 2$  or  $\leq -2$  were set as the threshold for significantly differential expression. Venn diagrams were made using VENNY ([http:// bioinfogp.cnb.csic.es/tools/venny/](http://bioinfogp.cnb.csic.es/tools/venny/)) with default settings. Heat maps were made using a platform from Biomarker Technology Co. GO analysis were made using DIVID 6.8 (Database for Annotation, Visualization and Integrated Discovery, <https://david.ncifcrf.gov/>) with default settings.

### **Chromatin immunoprecipitation PCR (ChIP-PCR)**

For ChIP-PCR assays, wild-type control and 35Spro-TCP5-Flag transgenic plants were grown under 20°C for 14 days after germination. Chromatins were sonicated to chip DNA into 200 bp to 500 bp fragments, and then were enriched by Anti-FLAG® M2 Magnetic Beads (Sigma). The DNA fragments was used as templates for qRT-PCR analysis. Relative levels of IP/Input was first normalized by *ACTIN8* (*ACT8*), and then was compared with input DNA samples.

### **QUANTIFICATION AND STATISTICAL ANALYSIS**

Statistical analyses were performed using Microsoft Office Excel 2016. Details of the statistical tests applied, including the statistical methods, number of replicates, mean and error bar details and significances, are indicated in the relevant figure legends. All replicates are biological, unless otherwise noted in the figure legend.